

**T-REX**  
**TERRAIN-INDUCED**  
**ROTOR EXPERIMENT**



**SCIENTIFIC OVERVIEW**  
**DOCUMENT**  
**AND EXPERIMENT DESIGN**

**December 2004**

**T-REX  
TERRAIN-INDUCED ROTOR EXPERIMENT  
OVERVIEW DOCUMENT  
AND EXPERIMENT DESIGN  
2004**

**Authored and Edited by**

Vanda Grubišić  
Desert Research Institute

James D. Doyle  
Naval Research Laboratory

Joachim Kuettner  
National Center for Atmospheric  
Research

Gregory S. Poulos  
National Center for Atmospheric  
Research

C. David Whiteman  
University of Utah

Contributing Authors:

L. Armi, B. Balsley, R. Banta, P. Brown, F. Chow, S. Cohn, W. Cotton, B. Demoz, S. DeWekker, A. Dörnbrack, D. Durran, S. Eckermann, D. Fritts, R. Frehlich, A. Heymsfield, R. Hertenstein, W. Hooper, J. Intrieri, Q. Jiang, M. Kaplan, G. Mayr, S. Mobbs, T. Lane, Y.-L. Lin, S. Mayor, Y. Meillier, S. Mobbs, L. Pan, R. Sharman, R. B. Smith, R. Street, S. Vosper, M. Weissmann, S. Zhong

Cover Picture: View of the Sierra Wave and rotor clouds over Owens Valley from a glider at 6,500 m. The uppermost wave cloud is at approximately 13,000 m, the smooth lenticular cloud at 10,000 m, and the rotor cloud reaches up to about 6,000 m. Wind is from the right (Photo: B. Woodward).

# T-REX OVERVIEW DOCUMENT AND EXPERIMENT DESIGN

## List of Contents

EXECUTIVE SUMMARY .....	1
1. Introduction .....	3
2. Scientific Objectives and Hypotheses .....	6
2.1 Dynamics and Structure of the Rotor Coupled System.....	6
2.2 Complementary Scientific Issues .....	10
2.3 Mesoscale and Microscale Modeling.....	13
2.4 Prediction of Aviation Hazards, Downslope Windstorms, and Aerosol Transport and Dispersion .....	16
3. Field Experiment Design and Observational Requirements .....	18
3.1 Project Phases .....	18
3.2 Observational Requirements and Strategy .....	19
3.3 Real-Time Numerical Modeling Support.....	23
4. Project Management Structure.....	24
5. Data Management Plan .....	24
6. Project Location and Operations.....	25
REFERENCES.....	26
APPENDIX: MAJOR FACILITIES AND INSTRUMENTATION .....	35
LIST OF TABLES .....	40
LIST OF FIGURES .....	41

## EXECUTIVE SUMMARY

The proposed Terrain-induced Rotor Experiment (T-REX) is the second phase of a coordinated effort to explore the structure and evolution of atmospheric rotors---intense low-level horizontal vortices that form along an axis parallel to, and downstream of, a mountain ridge crest---as well as associated phenomena in complex terrain. The initial, exploratory, phase of this effort, the Sierra Rotors Project, smaller in its scientific objectives and observational scope, completed its Special Observation Period (SOP) in early spring 2004 in Owens Valley, California. Experience gained and data collected in the Phase I SOP have been instrumental in formulating both the scientific objectives and experimental design of T-REX presented here.

Recent theoretical studies and observations of rotors, including the Phase I observations, show that rotors are strongly coupled to both the structure and evolution of overlying mountain waves and the underlying boundary layer. Although it is well known that atmospheric rotors pose a great hazard to aviation, there have been only a few studies of limited scope and no comprehensive studies of this important phenomenon in the last 30 years. Despite the significance of rotors, the studies have been so scarce because a comprehensive approach to the complex coupled system necessary to understand rotors has become possible only recently as a result of the newest advances in remote sensing technology, atmospheric numerical modeling, and our understanding of boundary-layer processes. Consequently, the *main scientific objective* proposed for T-REX is *a comprehensive study of the coupled mountain-wave/rotor/boundary-layer system*. This document presents an overview of the T-REX scientific objectives and an exposé of its experimental design.

In order to achieve its main scientific objective, the T-REX program has two main observational thrusts:

- ❑ Comprehensive ground-based and airborne, *in situ* and remote sensing measurements during strongly perturbed conditions favoring rotor formation, and
- ❑ Comprehensive observations of complex-terrain boundary layer structure and evolution from undisturbed to strongly perturbed conditions.

All field activities will be actively supported by a real-time dedicated numerical modeling effort. In addition to advancing the main scientific objective, T-REX data sets and findings are expected to yield further significant improvements in:

- ❑ Mesoscale and microscale modeling, and
- ❑ Prediction of aviation hazards, downslope windstorms, and aerosol transport and dispersion.

T-REX field activities will take place in Owens Valley in March and April 2006. Owens Valley lies to the east of the southern Sierra Nevada, which is the tallest, steepest, quasi two-dimensional topographic barrier in the contiguous United States. Mountain waves and attendant rotors are known to reach particularly striking amplitude and strength there. Climatological studies, including results from Phase I, show that the months of March and April have the highest frequency of rotor events. Ground-based and airborne, *in situ* and remote-sensing measurements will be conducted both upwind and within Owens Valley during the two month

period. This comprehensive set of measurements has been designed to document the three-dimensional nature of the coupled mountain-wave/rotor/boundary-layer system in unprecedented detail. The heterogeneous physiographic characteristics and locally severe relief in and upwind of Owens Valley require a tightly coordinated experimental design, which draws substantially from the early meteorological field campaigns in Owens Valley and the recent Phase I activities.

The experiment design presented in this document calls for a comprehensive observing system composed of US and European instrumentation platforms listed in the Appendix. The field operations will be supported by real-time mesoscale model forecasts, and ensuing field research will be tightly coupled with numerical modeling studies. Participants in this project include investigators from a large number of US universities and agencies, the National Center for Atmospheric Research, and several European universities and research institutes. They are listed in Table 1.

# 1. Introduction

Meteorological processes in mountainous regions are complex in nature and impact a broad range of human activities. Under strong wind conditions, atmospheric rotors accompanying mountain waves and windstorms can be serious hazards to air and ground transportation, and such windstorms can loft large amounts of dust and other particulate matter into the atmosphere. In particular, rotors have been cited as contributing to cases of aircraft upsets and accidents involving commercial, military and civilian aviation (Carney et al. 1995). Despite their considerable impact on human activity, some basic questions about rotors remain unanswered. Our knowledge of rotor size, internal structure, turbulence intensity, and predictability is still limited.

In the meteorological literature, the first references to atmospheric rotors date back to the 1920s and 1930s (Koschmieder 1920; Kuettner 1938) and describe this phenomenon in relation to the attendant lee waves. Several early field investigations employing airborne measurements, whose findings to a large degree still form the basis of what we know today about rotors, were conducted in the 1950s in the lee of the Sierra Nevada (Sierra Wave Project: Holmboe and Klieforth 1957; Grubišić and Lewis 2004) and in the 1970s on the Colorado Front Range (Colorado Lee Wave Program: Lilly and Toutenhoofd 1969; Lester and Fingerhut 1974). In particular, the Owens Valley-based Sierra Wave Project was the first to focus scientific interest on the intrinsic relationship between large-amplitude mountain waves and rotors. In the intervening thirty years, however, there have been no comprehensive studies of this important phenomenon, in part because rotors, with their high degree of intermittency, are dangerous and difficult to sample using *in situ* aircraft measurements, and also because they are too small in spatial scale to be routinely sampled by conventional observing networks. Recent theoretical studies and observations of rotors show that rotors are coupled to both the structure and evolution of overlying mountain waves as well as the underlying boundary layer. Studies of such complex coupled systems have not been feasible until recently.

With the latest advances in ground-based and airborne remote-sensing instrumentation, it has now become possible to document rotors, sub-rotor structures and zones of upper-level gravity wave breaking with remote sensors (Clark et al. 1994, 2000; Ralph et al. 1997). It has also only recently become possible to study the coupled boundary-layer processes in complex terrain in sufficient detail. On the modeling side, afforded by continuous advancements in high-performance computing, three-dimensional (3-D) numerical simulations of rotors with non-hydrostatic mesoscale models are now becoming possible at the high horizontal resolutions needed to numerically resolve them (Clark et al. 2000; Doyle and Durran 2002, 2004a,b; Vosper 2004; Chen et al. 2004a; Grubišić 2005).

In response to these new developments in instrumentation, analysis techniques, and numerical modeling, a two-phase coordinated effort has been undertaken by a group of US and European scientists to revisit the Sierra Nevada to unravel the underlying dynamical processes and relations between large-amplitude mountain waves, rotors and the boundary layer. Phase I of this effort, the Sierra Rotors Project, is currently underway. It was undertaken in part to collect climatological data on atmospheric circulations in Owens Valley, in preparation for the more extensive experiment proposed here. The Phase I Special Observation Period (SOP) took

place in early spring 2004, and the data collected during this SOP has been instrumental in formulating both the scientific objectives and experimental design of Phase II, the Terrain-induced Rotor Experiment (T-REX).

Proposed for T-REX is a unified scientific view and experimental design for simultaneous and comprehensive documentation of all elements of the coupled mountain-wave/rotor/boundary-layer system. Because rotors are strongly tied to the evolution of the boundary layer in complex terrain, outstanding scientific questions regarding the complex-terrain boundary layer, its phenomena, and exchange processes need to be and can be studied in conjunction with the mountain wave and rotor studies. The T-REX field campaign offers an opportunity to study both the coupling of the mountain-wave/rotor/boundary-layer dynamics during rotor events as well as the evolution of the boundary layer during transitional, low-wind, or quiescent periods. As experience from the Phase I field operations (Grubišić and Kuettner 2004) and initial satellite climatology findings show (Grubišić and Cardon 2002), there are likely to be many days without waves and rotors when quiescent to moderately disturbed boundary layers can be efficiently studied. Understanding the state of the atmosphere when rotors are not present is an important starting point in the study of rotor development. Furthermore, the study of quiescent boundary layers may provide important insight into mountain wave and rotor dynamics given the emerging significance of weak or stagnant flow in the lee-side boundary layer that may result in absorption of gravity wave energy (Smith et al. 2002, 2005; Jiang et al. 2005).

Under weaker-wind conditions, understanding atmospheric transport is also critical to applications that include air quality, fire weather, and emergency response, as well as minimum temperature forecasts for agricultural and industrial applications. A lack of pertinent and focused measurements in high mountainous regions, however, hinders our understanding and ability to confidently model complex-terrain boundary layer processes and evolution. The important physical processes under weaker-wind conditions are strongly tied to the diurnal heating and cooling cycle at the earth's surface, which drives thermally-forced flow systems (Whiteman 1990, 2000), and to the dependence of these systems on larger-scale winds aloft, pressure gradients, and cloudiness. T-REX offers a unique opportunity to apply new observational technologies to achieve improvements in the understanding and modeling of these physical processes. Recent advances in understanding and in studying these processes at night have been made in the Vertical Transport and Mixing experiment (VTMX; Doran et al 2002, Banta et al. 2004), in which a mixture of traditional and newer observational technologies was used successfully to document flow structures in a wide basin. T-REX offers an opportunity to test how well these findings can be generalized to a different terrain, and consequently further advance our understanding of these wind systems and hone our ability to model thermally forced flows.

The location of the T-REX field activities will be Owens Valley, which lies in the immediate lee of the southern Sierra Nevada (Figure 1). The Sierra Nevada is a north-northwest to south-southeast oriented mountain range of about 600 km length, 100 km width and a very compact ridgeline with a number of peaks above 4 km. The tallest peak (Mt. Whitney; 4,417 m), as well as the steepest orographic gradient in the contiguous United States, are located in its southern part. The Sierra Nevada generates many orographically induced phenomena in the atmosphere that are also encountered in the vicinity of other mountain ranges world wide, but it

is best known, perhaps, for the Sierra Wave, a large-amplitude stationary internal-gravity wave that, under favorable atmospheric conditions, forms above its steep lee slopes. The Sierra Wave was the primary subject of investigation in the 1950s Sierra Wave Project (Holmboe and Klieforth 1957). Owens Valley, located between the tallest and steepest portion of the Sierra Nevada to the west and the White-Inyo mountain range to the east, is the location where mountain waves and the attendant rotors are known to achieve particularly striking amplitude and strength. The valley itself is about 150 km long and 15-30 km wide and oriented approximately north to south. The average elevation change between the Sierra crest and the valley floor is roughly 3,000 m (Powell and Klieforth 1991). Pronounced diurnal wind circulations, channeled flows, and cold pools have also been documented on non-wave days in this valley during the Phase I field effort. The largest source of fugitive dust in the Western Hemisphere (the 280 km<sup>2</sup> dry Owens Lake bed) is located at the southern end of Owens Valley, and is the result of the diversion of tributaries of the Owens River into the Los Angeles Aqueduct beginning in the 1920s. In strong wind and rotor events, up to 70 tons of dust can be blown from the lakebed per second, generating dust storms in Owens Valley in which PM<sub>10</sub> concentrations have reached 40,000 µg m<sup>-3</sup> (Raloff 2001).

The March-April time frame is best suited for the entirety of the T-REX scientific objectives because the position of the boundary between the polar and subtropical jets provides the optimal conditions for development of large-amplitude mountain waves and rotors (Holmboe and Klieforth 1957) as suggested by a recent cloud satellite climatology (Grubišić and Cardon 2002; Figure 2). Together, March and April include many days with conditions favorable for generation of mountain waves and rotors and also many days when it will be possible to document terrain-induced boundary-layer circulations in Owens Valley under more quiescent conditions.

T-REX addresses a large number of scientific objectives that involve spatial and temporal scales ranging from microscale to the scale of the entire Sierra Nevada mountain range, and extend from the ground up to the upper-tropospheric/lower-stratospheric altitudes. The following text provides an *overview* of scientific objectives and hypotheses that will be addressed in T-REX. Detailed reviews of the scientific issues and justifications of specific scientific objectives will be left to the individual scientific proposals from T-REX participants.



## 2. Scientific Objectives and Hypotheses

A lack of scientific understanding of the structure, characteristics and evolution of the rotor and related phenomena exists for at least two reasons: 1) observational data about rotor internal circulations are practically nonexistent, and 2) rotors cannot be studied in isolation, as they are part of a complex mountain-wave/rotor/boundary-layer coupled system. T-REX is designed to comprehensively study all parts of this system including the interactions among the processes.

The scientific objectives of T-REX are the result of scientific priorities formulated in a series of T-REX planning meetings held over the last four years, involving a large number of scientists and organizations, and representing a considerable cross-section of the mountain meteorology and other atmospheric science communities. These objectives are listed in Table 2. They express the primary need to improve the understanding of: I) *Dynamics and structure of the rotor coupled system (Section 2.1)*, and in addition include a set of scientific objectives related to II) *Complementary scientific issues (Section 2.2)*, such as stratospheric-tropospheric exchange and structure and evolution of the complex terrain boundary layer in the absence of rotors. The comprehensive T-REX data sets will represent a unique test bed for validation of numerical models, and are expected to be instrumental in achieving further significant improvements in: III) *Mesoscale and microscale modeling (Section 2.3)* and IV) *Prediction of aviation hazards, downslope windstorms, and aerosol transport and dispersion (Section 2.4)*.

### 2.1 Dynamics and Structure of the Rotor Coupled System

#### *(A) The role of upstream flow properties*

It is well known from theoretical, numerical and laboratory studies of airflow past complex terrain that the properties of the incoming air stream, such as the profiles of wind, temperature, and moisture, and their variation with time, determine the basic characteristics of the dynamical response to airflow over an obstacle (Lyra 1943; Scorer 1949; Corby 1954; Scorer and Klieforth 1959; Queney et al. 1960; Ralph et al. 1997).

Mountain-wave/rotor systems, primarily a cold-season phenomenon in the Sierra Nevada, are usually associated with two distinctive tropospheric airstreams: a lower one consisting of a cold and moist air mass overflowing the mountain range and pouring down the lee slope (Figure 3), and a drier upper airflow containing a tropospheric wind maximum. These two airstreams tend to be separated by a sharp inversion (order of 10 K in strong rotor conditions), often made visible by the so-called “cap cloud”, and presumably representing an essential part of the fully developed wave/rotor system (Holmboe and Klieforth 1957). Recent observational and numerical studies indicate that the properties of this upstream inversion, including its strength, depth, and the wind shear across it, play a significant role in determining the rotor types and their intensity, as well as the lee wave structure above the rotor (Hertenstein and Kuettnner 2005; Mobbs et al. 2004; Vosper 2004). Changes in the approaching flow related to jet stream movements and their fine structure (‘jetlets’) are also thought to affect the character of the waves and, possibly, rotors. Initial hypotheses concerning this relationship, developed in the Sierra Wave Project (Holmboe and Klieforth 1957) need further testing.

Recent numerical studies have suggested that rotors are associated with boundary layer separation (e.g., Doyle and Durran 2002). However, the sensitivity of boundary layer separation to the upstream flow characteristics, such as the degree of upwind flow blocking as indicated by the formation of the sharp temperature inversion near mountaintop level, and the location and strength of the inversion has yet to be established.

The characteristics of the upstream moisture and latent heating profiles may also influence the resonant mountain wave response (Doyle and Smith 2003), as well as the rotor structure. In the upslope region, moisture will help the flow rise over the mountains. In addition, where clouds form over the windward slope, the input of solar energy at the underlying ground is reduced. Some evidence shows that the associated time-varying solar radiation and sensible-heat fluxes on the windward slope can affect the characteristics of the mountain waves and rotors downstream. The precipitation efficiency of the clouds on the windward slope will also determine how much evaporative cooling occurs when the air begins to descend, and how dry the downstream regions will be.

Consequently, one of the key T-REX objectives is to document the role of the upwind atmospheric structure, including the upstream temperature, wind, water vapor and latent heat release profiles, on the evolution of the rotor coupled system by employing a comprehensive set of ground observing systems and complementary airborne observations.

*(B) Wave/rotor dynamic interactions*

The causal relationship between mountain waves and rotors has never been systematically investigated. Limited observations of rotors in Owens Valley and other locations worldwide motivates the hypothesis that at least two types of rotors exist: Type I that forms underneath the crest of a mountain wave, and a rare Type II that bears a strong resemblance to an internal hydraulic jump (Figure 4). Because of the relatively few observations of rotors, the characterization of the mountain wave/rotor system as “wave-induced rotors” or as “rotor-induced waves” is clearly premature at this point. The existence of a relationship between wave amplitude and rotor strength has been documented in recent numerical experimentation (e.g., Doyle and Durran 2002). A possibility that rotors are conditioned by the characteristics of the capping inversion has been also been suggested by idealized numerical simulations (Figure 5; Hertenstein and Kuettnner 2005). The planned comprehensive ground-based and airborne observations in T-REX offer an unprecedented opportunity to examine these issues, including the dynamics and causality of this relationship, and to verify the existence of the hypothesized two rotor types.

Recent laboratory and numerical studies of mountain wave dynamics have emphasized the importance of 3-D effects, such as the span-wise variations of the gravity wave structure, on the rotor and breaking gravity-wave turbulence characteristics and strength (Gheusi et al. 2000; Clark et al. 2000; Doyle and Durran 2004b; Chen et al. 2004a), as illustrated by the numerical simulation shown in Figure 6. While the Sierra Nevada, particularly its southern portion, has a pronounced two-dimensional geometry, sufficient variation of the terrain features and height exists along the length of Owens Valley to induce span-wise variations of the mountain wave and rotor structure, and allow hypotheses related to the 3-D effects to be tested.

Additionally, as Owens Valley is located between two high parallel mountain ranges, T-REX offers an opportunity to investigate the effect of the downstream mountain range in determining atmospheric resonance conditions necessary for establishment of different types of mountain waves and rotors.

*(C) Internal rotor structure*

It is well known that the wind distribution within a tornado funnel may be highly non-uniform due to the presence of suction vortices (Fujita 1989). Ultra-high-resolution 2- and 3-D numerical simulations suggest that small intense horizontal vortices, the so-called “subrotors”, also form within atmospheric rotors (Doyle and Durran 2004a,b), when a vortex sheet, formed by surface friction beneath the layer of strong winds, lifts off the lee slope of the mountain and rises into the leading edge of the rotor (Figure 6). Numerical simulations suggest that the subrotors are generated along the rotor interface in a zone of large wind shear. The nature and characteristics of this instability has yet to be explored. The extent to which subrotors constitute a danger to aviation clearly depends on their strength, size, and longevity. Unfortunately, these basic subrotor characteristics are not currently known because of a lack of observational data. Additionally, the relationship between the subrotors and the rotor itself has yet to be established. Since the simulated subrotors are sensitive to the subgrid-scale turbulence parameterization used in the numerical simulation, and the faithfulness of such parameterizations is highly uncertain, the numerical results need observational verification. Advances in remote-sensing technology (lidars and K-band radars) now make it possible to document behavior of the subrotors. Doppler lidar, in particular, has proven to be an effective tool for studying flows in mountainous and other complex terrain, including mountain waves and windstorms (e.g., Neiman et al. 1988; Banta et al. 1990; Clark et al. 1994, 2000). Doppler lidar has also been found to be an important tool for documenting the structure and the temporal variability of the jump-like structures and wind reversals---indicators of rotors. Examples include near-surface (e.g., Figure 7, from Banta et al. 1990; also Weissmann et al. 2004) and upper-tropospheric (Clark et al. 2000) wind reversals.

*(D) Rotor/boundary-layer interactions*

The close coupling of the elements of the rotor system are supported by previous findings that mountain wave and rotor characteristics depend on surface friction, mechanical shear and surface heat flux above the lee slope (Richard et al. 1989; Doyle and Durran 2002). A vortex sheet, formed by surface friction beneath the layer of strong winds, lifts off the lee slope of the mountain and rises into a leading edge of the rotor. This lift is due to the boundary layer separation that occurs in connection with adverse pressure gradients on the lee side of the barrier (Doyle and Durran 2002). Model simulations also indicate that mountain waves and rotors may undergo distinct diurnal cycles in wavelength, strength and depth (Holmboe and Klieforth 1957; Ralph et al. 1997; Kuettner and Hertenstein 2002; Doyle and Durran 2002; Chen et al. 2004b) in response to diurnal boundary-layer forcing. Additionally, in a lee-side valley such as Owens Valley, the evolution of waves and rotors will depend on the interaction with the pre-existing boundary layer in the valley (Kuettner 1939; Poulos 1996; Poulos et al. 2000). The existence there of a cold air pool (Whiteman et al. 2000), a convective or neutral boundary layer (CBL or NBL), or thermally driven (Whiteman 1990; Stewart et al. 2002) or channeled winds (Gross and Wippermann 1987; Whiteman and Doran 1993) can be expected to

affect this development. Additionally, topographic and surface cover irregularities including soil characteristics may play a role in determining the locations of boundary-layer separation and thus strongly affect rotor initiation and maintenance.

Surface heating along the lee slope has been hypothesized to increase the intensity of the rotor, based on observational and theoretical considerations (e.g., Kuettner 1959) and numerical simulations (e.g. Doyle and Durran 2002). Furthermore, documentation of the entrainment impact on rotors along internal hydraulic jumps and the effect of downslope flow entering either a denser cold pool or less dense air mass (e.g. due to a heating during the afternoon hours; Kuettner 1959) are issues that need to be resolved and are related to the more general topic of turbulent mixing in internal hydraulic jumps. The attendant theoretical and observational study of entrainment effects across the density step of the atmospheric internal hydraulic jump would extend the results of Pawlak and Armi (2000), and offer an opportunity to consolidate them with existing laboratory (cf. Armi, 1986) and numerical studies on mixing in internal hydraulic jumps and rotors.

Using dense arrays of surface meteorological towers and microbarographs for detecting adverse pressure gradients, surface-based remote sensing, and flux towers, T-REX offers an opportunity to investigate the degree to which surface boundary-layer properties, such as heat, momentum and moisture fluxes, roughness lengths, and CBL/NBL depth, determine the characteristics of rotors, including separation, rotor strengths and depths, the strength of reversed flows at the surface, and the state of the mountain-wave/rotor/boundary-layer system coupling. This will allow us to answer fundamental questions such as whether the hypothesized Type II rotors are simply a response of the free atmosphere to the boundary layer separation at a hydraulic jump, or whether the rotor is part of a more complex free atmosphere wave/rotor system generated by the mountains and the separation is a boundary layer response to the rotor.

The presence of the large source of fugitive dust at the southern end of Owens Valley (the dry Owens Lake bed) provides unparalleled opportunities to utilize scanning Doppler and aerosol lidars to sample the 3-D structure of the rotor coupled system, and provide an important impetus to quantifying the role of mountain-wave-associated downslope windstorms on aerosol transport and diffusion from Owens Valley.

#### *(E) Upper-tropospheric wave breaking and turbulence*

Observational studies have shown that mountainous regions are a preferred location for clear-air turbulence in the upper troposphere (Reiter and Foltz 1967). The question remains, however, as to what exact circumstances lead to clear-air turbulence at upper-tropospheric and lower-stratospheric levels (~6-14 km) above complex terrain. Mountain wave breaking and related turbulence should be enhanced above jet streaks in layers of strongly reversed shear and suppressed below the jet stream within the forward shear region. However, relatively little is known regarding the role of jet streams and their interaction with mountain waves and wave breakdown (e.g., Clark et al. 2000), in part because of a lack of systematic observations. The Sierra Nevada is a quasi-two dimensional barrier with a steep lee-side slope that is an ideal natural laboratory for studying the lifecycle of mountain waves including generation, amplification, instabilities, wave breakdown and transition to turbulence, and their interaction with the mean flow (Figure 8). Gaining better understanding of conditions associated with the

processes governing mountain waves and the nature of the life cycle of turbulence associated with these waves is a critical need in better characterizing gravity wave (GW) influences in the lower, middle, and upper atmosphere because of the significant role played by orographic GWs globally (Ehernberger 1987; Nastrom and Fritts 1992; Eckermann and Preusse 1999; Stefanutti et al. 1999).

*In situ* documentation and remotely sensed characterization of turbulence by research aircraft, along with fine-scale simulations (initialized and validated by a suite of aircraft and ground-based observations), are expected to yield improved insight into the character of turbulence, including its intensity and intermittency, and to aid in assessing the influences of instability dynamics in the troposphere and stratosphere on mountain wave and rotor structure and its variability. The observations, tested against predictions from various mountain-wave turbulence algorithms and numerical simulations [e.g., Clark-Hall model (Clark 1977), EULAG (Smolarkiewicz and Margolin 1997), Mountain Wave Forecasting Model (Eckermann et al. 2004), COAMPS<sup>TM</sup> (Hodur 1997), RAMS (Pielke et al. 1992), UK Met Office Unified Model (Cullen 1993), and the Weather Research and Forecasting (WRF) model], can be used to evaluate current parameterizations of orographic gravity wave drag (GWD) (Fritts and Alexander 2003; Kim et al. 2003) and motivate new approaches to orographic GWD representations in climate and global NWP models. The application of several different numerical models to mountain-wave induced turbulence will lend much needed new insight into the predictability of turbulence-related aviation hazards (Doyle et al. 2000) and will test the capability and skill of multi-model approaches to forecast wave-induced turbulence in a manner analogous to multi-model ensembles of tropical cyclones, which have been demonstrated to be more skillful than any single member (e.g., Goerss 2000).

## 2.2 Complementary Scientific Issues

### (A) Stratosphere-troposphere exchange

Stratosphere-troposphere exchange (STE) is a key factor controlling trace gas distributions in the upper troposphere and lower stratosphere (Holton et al. 1995; Stohl et al. 2003). High-resolution *in situ* aircraft observations have shown that mixing of chemical constituents is often associated with gravity waves near jets (e.g., Cho et al. 1999; Pavelin et al. 2002). The extent to which vertical redistribution of tracers can be caused by large amplitude (possibly breaking) mountain waves has not been previously documented. Aircraft observations of stratospheric and tropospheric tracers (e.g., O<sub>3</sub> and CO) in conjunction with other *in situ* and remote sensing aircraft measurements by high-altitude aircraft in T-REX, primarily NSF HIAPER (cf. Table 3), offer an opportunity to quantify mountain wave contributions to stratosphere-troposphere exchange processes and answer questions such as: i) how deep are vertical intrusions of tropospheric air into the stratosphere associated with stable wave motions in a reversible process, ii) what are the details of the irreversible mixing associated with mountain wave breaking, and iii) is the mixing occurring at the right level to induce significant stratosphere-troposphere exchange? We plan to pursue this objective by a set of chemical tracer measurements on board the HIAPER aircraft in conjunction with an upward looking ozone lidar on board UK BAe146. These chemical measurements will provide the first direct observation of the contribution of mountain waves to STE. They will also provide additional information about

the effect of the coupled rotor system on air motions at the upper levels, therefore supporting the main objective of the experiment. In addition to measurements, models that are capable of simulating transport and mixing in a range of scales from planetary- to mesoscales will be used to help interpret data. A separate funding application to the UK Natural Environment Research Council by University of Leeds scientists aims also to ensure that the UK BAe 146 aircraft (Table 3) will be equipped with chemistry instrumentation including an upward and downward looking ozone lidar to address related objectives concerned with vertical mixing of constituents by rotors and mountain waves.

*(B) Boundary-layer structure and evolution in absence of rotors*

Documenting the state of the atmosphere within Owens Valley on non-wave/rotor days is critical for achieving the central set of T-REX objectives as it will establish a foundation from which to study rotor/boundary-layer interactions. For example, during an event in Phase I a build up of strong convection was observed over the high Sierra peaks with descent over Owens Valley and easterly flows within the valley. As easterly flows can also be associated with rotors, such non-wave events must be well understood, predicted and interpreted. In addition, in order to clearly identify the influence of the boundary layer on rotor development as well as the effect of rotors on the boundary layer, it is essential to characterize the boundary layer structure within the valley in the absence of rotors.

For many combinations of cross-barrier wind profile, upstream temperature inversion structure and height, surface heating, and other external factors that may define a parameter space, wave and/or rotor responses are likely to be absent. Indeed, satellite- and surface-tower-array-based climatological investigations from Phase I show that there are likely to be many non-mountain-wave days when a quiescent to moderately disturbed diurnal boundary layer exists in the valley (Grubišić and Cardon 2002; Grubišić and Kuettner 2004). The proposed two-month T-REX deployment has therefore been designed to address a range of hypotheses on boundary- and surface-layer development in Owens Valley during quiescent non-wave/rotor periods and during transitions from quiescent to disturbed periods. Specifically, this effort will further our aim to understand: 1) how surface features act to control the location of rotor separation and reattachment, and 2) how is the flow separation and the strength of rotors influenced by surface sensible heat flux.

Some of the same features that make Owens Valley suitable for the study of rotors, contribute to its suitability for studying complex terrain phenomena in the absence of rotors. With its long, narrow and steep-walled configuration, semi-arid climate and minor influences from tributary valleys, urban areas, lake and sea breezes, Owens Valley represents a relatively simple natural laboratory, where valley thermal forcing and channeling effects are expected to be relatively pure. In such a semi-arid environment, a large fraction of the net radiation is converted to sensible heat flux. Outgoing radiation at night and incoming radiation during daytime cause strong diurnal variations in the boundary layer structure, and the formation of well developed thermally driven flows documented in Phase I (Figure 9). Consequently, this relatively idealized natural laboratory provides a unique environment to study boundary layer processes and thermally forced flows to be compared to documented processes and flows in other valleys of the arid Western United States with different geometries, including the Salt Lake basin (Banta et al. 2004, Doran et al. 2002), the Grand Canyon (Whiteman et al. 1999a,b;

Banta et al. 1999), and other valleys in Colorado (Whiteman 1982, King 1997, Post and Neff 1986, Banta and Cotton 1981, Banta 1986).

A number of boundary layer processes in valley settings remain poorly understood. For example, as ridge-top wind speeds increase or as surface-based heating (during daytime) increases, processes such as topographic channeling (Whiteman 1990) and downward mixing of momentum (Banta and Cotton 1981; Banta 1986) can significantly alter flow in valleys. Ridge-top-wind and wave-induced-turbulence effects on nighttime drainage flows, cold-pool erosion, asymmetric heating of valley sidewalls, and along-valley variability have been shown to have strong influences on in-valley flows in many parts of the world, but responsible dynamical processes have not been well characterized. Studying these effects with the instrumentation available during T-REX will provide an excellent opportunity to understand mechanisms responsible for these interactions.

Applying the proposed comprehensive deployment of instrumentation to this setting will provide an unprecedented opportunity to understand other important components of the complex terrain boundary layer. This includes phenomena such as layered structure of the flow under statically ( $Ri > 0$ ) and dynamically ( $Ri > 0.25$ ) stable conditions, as well as inversion creation, breakup and turbulent erosion. Of special interest is the development of spatially resolved mean flow, surface flux, and flux profile data sets that can be used to test the surface- and boundary-layer theories. The existing theories were developed using flat terrain measurements (Elliot 1964, Oke 1970, Webb 1970, Businger et al. 1971, Businger 1973, Carson and Richards 1978, Kondo et al. 1978, Louis 1979) but used widely over complex terrain, leading to significant parameterization errors (Derbyshire 1999; Mahrt 1998a,b; Poulos et al. 2002; Poulos and Burns 2003; Van de Weil 2002a,b, 2003; Chow et al. 2005). While it has been shown that in statically stable conditions various boundary layer parameterizations fail to capture the impact of intermittent turbulence on heat and momentum transport in relatively flat terrain (Poulos and Burns 2003), a comprehensive representation of underlying physical processes requires measurements at sites with varying physiographic characteristics.

Such data obtained in T-REX, will be crucial for verifying large-eddy simulation and high-resolution mesoscale numerical modeling of the complex terrain boundary layer (cf. Section 2.3), and characterizing the heterogeneity of surface/boundary layer statistics caused by physiographic heterogeneity or intermittent turbulence with varied non-local sources, including overlying rotors. In addition, the vertical profile of turbulence in the boundary layer has been recently shown to play a central role in wave absorption by boundary layer and in boundary layer stagnation that might be triggering rotors (Smith et al. 2005).

During both daytime and nighttime in relatively quiescent periods, the investigation of the temporal and spatial variability of atmospheric boundary layer (ABL) and aerosol layer (AL) heights is also of interest. As opposed to the assumptions in standard dispersion calculations, recent investigations have shown that there is a distinct difference between ABL and AL heights in mountainous terrain (De Wekker et al. 2004), caused to a large extent by mountain venting and relatively complex terrain-specific boundary layer entrainment processes (Kossmann et al. 1999). For the transport of dust on a regional to continental scale, the aerosol layer height is a critical parameter, yet its behavior over mountainous terrain is poorly understood. The unique and comprehensive measurements proposed for T-REX would allow an assessment of the role

of rotors, other mountain wave induced turbulence and complex terrain flows in the exchange of aerosols between the boundary layer and the troposphere above.

*(C) Wave cloud phase transitions and layering*

The process of ice nucleation is of central importance to meteorologists from both the observational and modeling communities. Wave clouds offer the best opportunity to study the phase-transition process because these clouds have relatively steady-state humidity and temperature structures, and the leading edge often has humidity close to or above water saturation (Figure 10). Anecdotal reports from glider pilots suggest that the leading edge of a wave cloud can contain liquid water at temperatures as low as  $-50^{\circ}\text{C}$ . With a depolarization lidar, upward or downward pointing, followed by *in situ* penetrations, one can examine, in much more detail than previously, possible environmental conditions in which the homogeneous freezing process occurs. MODIS imagery can also be used to distinguish between ice and liquid clouds (King et al. 2004). In addition to conditions related to homogenous ice nucleation, measurements in wave clouds in Owens Valley offer an opportunity to determine the physical and chemical characteristic of aerosols entering the upwind side of the cloud, and the state of mixing of insoluble components of aerosols with the cloud droplets in the supercooled liquid cloud.

Wave clouds are often observed as thin horizontal layers, separated in the vertical by cloud-free air; the appearance is similar to a “stack of plates” (Figure 10) The conventional thinking is that the fine layering of the wave clouds may be a property of the upstream humidity field, although thermodynamic stability may also play a role. In T-REX we propose to investigate the process responsible for wave cloud layering by using a tunable diode laser hygrometer and a high-response temperature probe onboard an aircraft.

## **2.3 Mesoscale and Microscale Modeling**

*(A) Predictability of rotors and wave breaking*

The rapid increase in computer power over the last decade has enabled a new generation of mesoscale numerical weather prediction models to be applied at ever-increasing horizontal and vertical resolutions. However, the predictability limits of many mesoscale phenomena have yet to be explored. The T-REX dataset and program will provide a unique opportunity to advance our understanding of the predictability of topographically forced phenomena such as mountain waves, mountain wave breaking, rotors, and embedded sub-rotor structures. The interplay between field measurements and high resolution simulations will lead also to deeper understanding of the actual physical processes in play, some of which are, as noted below, not fully understood.

It has long been recognized that upstream properties of the flow, such as the static stability and incident wind speed, have an important influence on the characteristics of the mountain wave response (e.g., Smith 1989; Durran 1986). It follows that the properties of the synoptic-scale flow, including the presence of inversions near the mountain top that may be conducive



for downslope windstorms and large-amplitude wave generation, will likely have an important impact on the predictability of the mountain waves and rotors. Radiosondes located upstream and downstream of the Sierra Nevada as well as dropsondes can be used to evaluate the performance of the numerical models and address some of these predictability issues. Additionally, the timing and evolution of synoptic-scale features such as fronts and jet streams are related to the formation of, and influence the predictability of mountain waves and rotors. Mesoscale variations within the large-scale flow, such as cross-mountain wind speed jets and spatial variability in inversion strength, also influence the wave and rotor response. During the Phase I effort, several real-time high-resolution numerical forecasts produced at consecutive initialization times exhibited considerable variability in the predicted strength of downslope winds, likely related to changes in the forecasted upstream flow characteristics. Thus, the uncertainties in the large-scale and mesoscale initial conditions and boundary conditions need to be assessed for these topographically forced flows.

Mountain wave breaking and rotor generation may be considered to be threshold phenomena (e.g., Smith 1989; Doyle and Durran 2002), and the predictability of such phenomena may not only be limited by the upstream flow properties, but also by nonlinearities associated with the mountain wave dynamics. In Phase I studies, the presence of wave breaking, rotors, and sub-rotors above the surface could not be easily deduced, because of a lack of remote sensing platforms with sufficient vertical resolution and horizontal coverage. As a result related mesoscale predictability issues could not be addressed. During T-REX, the use of upstream radiosonde observations in concert with remote sensing instrumentation, such as Doppler lidars located on the lee side, will provide an excellent opportunity to explore the intrinsic predictability of turbulent characteristics of the flows, such as boundary layer separation, low-level wave breaking, rotor, and sub-rotor development.

Uncertainties in the model formulations, specifically the dynamic cores and physical parameterizations such as boundary layer and turbulence schemes, also likely contribute to predictability limitations (Bright and Mullen 2002). These predictability issues can be explored using the T-REX observations and a suite of modeling approaches that include high-resolution model sensitivity experiments with real-data and idealized initial states, mesoscale ensembles, and adjoint models (see e.g., Langland et al. 1996).

#### *(B) Subgrid-scale parameterization issues*

The representation of sub-grid scale processes such as turbulent mixing and fluxes within the boundary layer, and microphysical processes within topographically forced clouds, are important research issues for numerical modeling on scales that extend from the microscale to global scale. The T-REX observational program will provide valuable datasets to evaluate subgrid-scale parameterizations in regions of complex topography for a variety of large-scale forcing conditions. For example, the impact of surface flux and boundary layer representations on topographically-forced phenomena, such as mountain waves, rotors and diurnally-forced flows, needs to be systematically explored. This is especially needed in light of previous studies that have demonstrated the sensitivity of mesoscale forecasts to boundary-layer characteristics associated with varying surface conditions such as vegetative properties and soil moisture (Chen et al. 2001). The soil moisture initialization, in particular, was crucial in accurately predicting slope-flow development (Banta and Gannon 1995) and valley wind transitions in large-eddy

simulations of flow in a steep and narrow Alpine valley (Chow 2004). The sensitivity to soil moisture in Owens Valley is expected to be most important during non-rotor and transition periods. Despite the fact that the valley lies in an arid region, variability in soil moisture between locations on the dry slopes versus those near the Owens River on the valley floor do exist. Soil moisture probes will be deployed throughout the valley to measure the variability of soil moisture and temperature along the valley floor, slopes, and near the crests of the surrounding mountains. In a related boundary layer issue, the representation of the stable boundary layer remains an open question because of a number of factors including intermittent turbulence, local instabilities, gravity waves, and microscale flows (see e.g., Mahrt and Vickers 2003). Above the boundary layer, the parameterization of turbulent mixing within wave breaking layers aloft in the troposphere and stratosphere needs to be evaluated using T-REX research aircraft measurements.

The representation of orographic drag in larger-scale numerical models remains a major challenge (Kim et al. 2003; Fritts and Alexander 2003), particularly with regard to boundary layer interactions with the flow and wave breaking. The results from high-resolution modeling together with observations collected during T-REX will serve as the foundation for much-needed next-generation approaches to gravity wave drag parameterization methods. A number of numerical modeling studies have suggested that wave breaking is diminished and strong lee-side winds are enhanced in the presence of surface friction (e.g., Richard et al. 1989; Ólafsson and Bougeault 1997), however many questions remain regarding boundary layer and surface interactions with mountain flows.

#### *(C) Representation of steep terrain*

The numerical representation of the steep topographic slopes of the eastern Sierra is also a severe test for mesoscale models and terrain transformations associated with these vertical coordinates. In order to properly represent airflow over and around terrain, nearly all mesoscale weather prediction models make use of a terrain-following coordinate. Previous studies have indicated that steep terrain may induce spurious accelerations because of truncation errors in the horizontal pressure gradient (Schär et al. 2002). However, observational data with sufficient resolution have been lacking to test the new-generation of high-resolution non-hydrostatic models for steep terrain flows. The ground-based and aircraft observations collected during T-REX will prove valuable in testing current and next-generation formulations for numerical model vertical coordinates. Although only a small portion of surface instrumentation will extend as far as the upstream crest, it is anticipated that sufficient measurements along the lee slope will be available to document the atmospheric properties of the flow, such as pressure and winds that can serve as benchmark cases for high-resolution numerical models applied in steep terrain.

#### *(D) Mesoscale verification*

Relatively few high-resolution models have been evaluated in complex terrain under both strong and weak forcing conditions, partly because of a lack of observations on complementary scales and representativeness issues of the measurements (e.g., Mass et al. 2002). The T-REX program will provide an excellent opportunity to validate and evaluate the performance of mesoscale and microscale models such as the Weather Research and Forecasting (WRF) model,

the Advanced Regional Prediction System (ARPS), and the Coupled Ocean/Atmosphere Mesoscale Prediction System (COAMPS), as well as linear modeling approaches (Smith et al. 2002; Broutman et al. 2003), all of which can be used for real-time predictions. These evaluations can be performed on a case study basis or for an extended period of time, since the T-REX automatic surface station network will be available over a multi-year period (cf. Section 3.1). Sensitivity studies need to be conducted with respect to the boundary and initial conditions, as well as to evaluate the performance of various representations of physical processes. The T-REX dataset also will be useful in testing new approaches and methodologies for mesoscale verification.

## **2.4 Prediction of Aviation Hazards, Downslope Windstorms, and Aerosol Transport and Dispersion**

### *(A) Aviation hazards*

Details of the internal structure of rotors are largely unknown because of a lack of direct observational data. Much of the existing knowledge about rotors is anecdotal, stemming from pilot reports after unplanned encounters with rotors. To our knowledge, the only penetration of a severe rotor by a fully instrumented aircraft (B-29) took place in the Sierra Wave Project in 1955. Recorded vertical gust (Figure 11), some on the order of  $\pm 20 \text{ m s}^{-1}$  over a very short time, imply strong eddies on the decameter scale. Most rotors contain at least moderate turbulence. While strong turbulence is not uncommon, extreme turbulence, which can lead to loss of control, is fortunately rare. One danger posed by rotors is potentially a sudden transition from smooth air in the lee wave to turbulence in the rotor. A pilot unfamiliar with rotor flow characteristics may not have time to reduce airspeed, and the aircraft load limits can be exceeded. This may have led to the 1992 in-flight breakup of a twin-engine aircraft reported by Carney et al (1995). Even at lower airspeeds, load limits can be inadvertently exceeded while flying through rotors. An example is the 1993 incident in Alaska in which a Boeing 747 lost one engine in rotor turbulence during departure. It is noteworthy that these events occurred at or below mountaintop level. Adding to the danger is the fact that rotors can occur in clear skies when visual clues may be entirely lacking. Even when rotor clouds do exist, they often are rather innocent looking to an untrained eye (e.g., Figure 4). In addition, strong shifting winds can occur when rotor circulations extend to the surface, leading to hazards for departing and landing aircraft (e.g., Mobbs et al. 2004). On the other hand, skilled pilots who are alerted to the likely presence of rotors and associated turbulence can take proper in flight actions and safely avoid the hazards.

The T-REX field program will offer a unique opportunity to improve the current capabilities for prediction of the potential for severe aviation turbulence in the lee of a major mountain range. Prediction of mountain wave turbulence is currently based on various empirical or semi-empirical algorithms. Experience from the application of mesoscale numerical models to real-time prediction of severe aviation turbulence has indicated that the nonlinear processes that induce turbulent motions can be inferred, in many cases, from certain mesoscale predictive indices that are very sensitive to the effects of terrain and moist convection on downstream mass and momentum perturbations (e.g., Kaplan et al. 2004a, b, c). The predictive skill of these and other similar indices can be tested against aircraft observations of turbulence using data

from remote observations with lidar, and *in situ* data and turbulence statistics from turbulence encounters. These observations will help improve the understanding of the life cycle of turbulence in mountain waves and test observations against ultra-high-resolution simulations with numerical models such as the Clark-Hall, EULAG, COAMPS, and the North Carolina State University adaptive grid version of MM5 (Xiao et al. 2005), which will be used to simulate processes resulting in the downscale organization of potential aviation turbulence in the lee of the Sierra Nevada. Support from the Federal Aviation Administration (FAA) Aviation Weather Research Program is anticipated for using T-REX observations to better understand and forecast mountain-wave related turbulence.

*(B) Downslope windstorms*

The operational forecasting of mountain wave activity and downslope winds relies on a blend of guidance from numerical models and empirical algorithms. Although empirical methods can be skillful in some regions and situations (e.g., Hopkins 1994), the algorithms are typically dependent on the local terrain and perform poorly with regard to the peak wind intensity. Operational numerical weather prediction of mountain waves and downslope winds is currently limited by a number of factors, many of which have yet to be explored (e.g., predictability), and coarse resolution that may lead to a misrepresentation of key terrain features. T-REX observations will aid in the evaluation of the forecasting capability of numerical models and the existing algorithms, and provide an excellent base for developing more generalized and physically-based forecasting algorithms capable of predicting the intensity of windstorms. Intercomparison of T-REX measurements with forecasts from different model types, the mesoscale models (COAMPS, RAMS, ARPS, WRF) and the mountain wave forecast models, is expected to yield improvements in individual model performance in forecasting mountain wave responses over the Sierra Nevada. This, in turn, is expected lead to improvements in operational forecasting of severe downslope winds and mountain-wave/rotor events in the lee of the Sierra Nevada and other mountain ranges.

*(C) Aerosol transport and dispersion*

The dry lake bed at the southern end of Owens Valley is a prodigious source of fugitive dust under mountain wave conditions. This dust contains large amounts of particulate matter that is 10  $\mu\text{m}$  in diameter or smaller ( $\text{PM}_{10}$ ) and contains high concentrations of cadmium, arsenic and other heavy metals that accumulated in the lake bed over time. During strong wind events, up to 70 tons of dust can be blown from the lakebed per second, generating dust storms in Owens Valley in which  $\text{PM}_{10}$  concentrations have reached 40,000  $\mu\text{g m}^{-3}$  (Raloff 2001). These concentrations far exceed federal air quality regulations, which prohibit the 24-h average  $\text{PM}_{10}$  concentration from exceeding 150  $\mu\text{g m}^{-3}$  more than once per year. Networks of weather stations and aerosol sampling equipment have already been deployed by other government agencies such as the State of California, the China Lake Naval Weapons Center, NOAA, EPA, and the USGS in Owens Valley mostly south of the T-REX observational area to investigate the transport and diffusion of this dust (Reheis 1997). Previous studies have emphasized aerosol collection, but they have lacked the level of meteorological support that will be part of the T-REX program (Gill and Gillette 1991; Cahill et al. 1994; Reheis 1997). The intensive meteorological measurements, analyses and modeling that will be conducted in T-REX are expected to add significantly to the research on fugitive dust emissions funded by other

agencies, and to provide an important impetus to studies of aerosol transport and diffusion from Owens Valley. Collaborations between T-REX and other investigators may result in interchanges of data and enhancement of the scientific results from both investigations. Of special research interest would be investigations of the role of mountain waves, rotors and associated downslope windstorms on total dust transport and diffusion.

### 3. Field Experiment Design and Observational Requirements

#### 3.1 Project Phases

T-REX is Phase II of the coordinated two-phase effort to explore the structure and evolution of atmospheric rotors and associated phenomena in complex terrain.

**Phase I** of this effort is the Sierra Rotors Project (SRP). The SRP Special Observation Period (SOP) took place in Owens Valley in March and April 2004 (Grubišić and Kuettner 2004). The goals of the Phase I effort have been, in part, to obtain climatological data on the locations and frequency of occurrence of rotors in Owens Valley to aide in the design of Phase II. The core instrumentation deployed consists of the DRI long-term network of 16 automatic weather stations (AWS) with telemetry located south of Independence in the central portion of Owens Valley. This network has been providing data in near real-time since the end of February 2004 (<http://www.wrcc.dri.edu/trex>), and will be part of the Phase II field instrumentation as well. The rest of instrumentation deployed includes two NCAR Integrated Sounding Systems (ISS), one with the Multiple Antenna Profiler (MAPR) and the other a mobile system (MISS), a time-lapse video system and an instrumented car in Owens Valley, and two atmospheric sounding systems (a mobile NCAR system (MGAOS) and a radiosonde unit at Naval Air Station (NAS) Lemoore) in the San Joaquin Valley upwind of the Sierra Nevada (Figure 12).

The number of wave events that occurred during the SOP is close to that expected from the past data on Sierra Wave occurrences in Owens Valley (cf. Figure 2). All documented rotor events appeared to be of Type I, and could be characterized as moderate to strong events (Figure 13). Some of the SRP wave events lasted for several days. During these multi-day events, the surface network documented a quasi-diurnal variation of the wind in the valley; the wind was easterly or southerly in the morning and early afternoon, shifting to westerly in the afternoon or late afternoon hours. The maximal surface gusts recorded by the ground network during wave events were in the range of 20 to 30 m s<sup>-1</sup>. One of these events (Intensive Observation Period 8 on March 25) was sufficiently strong for the reversal (easterly flow) at the ground to reach 4 m s<sup>-1</sup> (Figure 14). High temporal and altitude resolution vertical velocity measurements by wind profilers showed cases of persistence over time as well as great variability in measured velocity during strong wave events (Figure 15; also Grubišić and Cohn 2004). Persistent features were also observed in the wind profiler Doppler spectra, which are related to velocity variance, i.e., turbulence. The northern line of AWS network and MISS, which was located at its northern end, have repeatedly experienced stronger winds compared to the rest of the network as well as MAPR located at its southern end. Consequently, in T-REX, additional ground-based instrumentation including surface stations, lidars and wind profilers will be placed to the north of the DRI network. As expected, the AWS network and the ISS

deployed in Phase I were sufficient only for the documentation of the strongest wave and rotor activity. A significant augmentation of the observing system in T-REX is needed in order to document the coupled rotor system under a wide range of wave/rotors strengths and conditions.

Phase I is still underway and will end with the onset of Phase II in spring 2006. Surface meteorological data from Owens Valley is being continuously received at DRI from the AWS network, and radiosonde launches continue on a case-by-case basis from NAS Lemoore.

**Phase II** is the two-month field phase described in this document, covering March and April 2006. During these two months, dedicated special observing systems will be deployed in Owens Valley, including research aircraft and ground-based instrumentation such as additional networks of AWS, temperature and soil-moisture sensors, ISS, Doppler and aerosol lidars, sodars, and various specially instrumented towers. Our recent activities in the Sierra Rotors Project indicate that the primary scientific aim of T-REX of documenting the rotor coupled system can be best achieved during these months, while also providing a sufficient number of relatively quiescent days for the study of the complex terrain boundary layer.

### **3.2 Observational Requirements and Strategy**

To adequately address the scientific goals reviewed above, many atmospheric phenomena need to be observed and measured during T-REX. Obtaining both surface and upper air measurements appears an imperative for understanding the rotor phenomenon and its internal structure, and the dynamical linkages of rotors with both the overlying mountain-wave and the underlying boundary-layer evolution and structure. A dense, ground-based network of instruments has been designed to work in concert with a suite of airborne measurement systems required for the documentation of the middle- and upper-levels of the rotor coupled system.

Owing to the cross-barrier and along-valley orientation of the atmospheric phenomena to be studied, both cross- and along-barrier sampling strategies will be used. Rather than providing single cross-sections, which will not adequately assess the multi-dimensional nature of the phenomena subject to our hypotheses, we have devised an optimized observational program that will provide measurements of the 3-D nature of the complex terrain phenomena, including surface heterogeneity. An important rationale for our strategy is the satisfactory initialization and verification of the detailed numerical modeling studies planned within the T-REX research program.

To measure the breadth of phenomena that are of scientific interest to T-REX both individually and collectively, we have devised a measurement strategy that combines both continuous and intermittent observations by a variety of instrument systems. Some of the planned measurements, by nature of the less frequent occurrence of the phenomena to be documented, will be met through intensive observational periods (IOP) (e.g. aircraft and manually-operated instrumentation), whereas others, especially those requiring the acquisition of robust statistics, will be met through continuous operation.

The T-REX observational strategy is comprised of two main observational thrusts:

- (1) Comprehensive ground-based and airborne, *in situ* and remote sensing measurements during strongly perturbed conditions favoring rotor formation, and
- (2) Comprehensive observations of complex-terrain boundary layer structure and evolution from undisturbed to strongly perturbed conditions.

*(1) Strongly perturbed conditions favoring rotor formation*

The primary method of observing the structure and evolution of the coupled mountain-wave/rotor/boundary-layer system under rotor conditions is based on utilizing the *in situ* and remote-sensing capabilities of research aircraft (Figures 16 and 17) in conjunction with ground-based instrument systems including lidars, wind profilers, sounding systems, dense networks of automatic weather stations and microbarographs, flux towers, and measurements from an instrumented car (Figure 18). In addition, time-lapse photography, GOES satellite imagery, and cloud cover will be collected continuously during the entire T-REX period.

Densely sampled thermodynamic and velocity data for documentation of airflow over Owens Valley as well as up- and downstream of the valley centerline will be obtained by research aircraft in cross-mountain traverses of up to 300 km in length as shown in Figure 16. The aircraft and their recommended height ranges are given in Table 3. The University of Wyoming King Air 200T will cover flight levels from the ground up to 28,000 ft, whereas the NSF/NCAR HIAPER will be used to reach upper-tropospheric/lower-stratospheric levels. The remote sensors on board the mid- and upper-air aircraft, primarily up- and down-looking lidars on board the UK BAe146 and HIAPER, the latter equipped with SABL or a new eye-safe lidar, will be the primary tools for documenting gravity wave breaking in clear air and turbulence within cloudless rotors. The capability of airborne lidars to document these turbulent zones will depend on the aerosol concentration within and over Owens Valley. The aerosol concentration is known to be high during strong wave events due to significant dust lifting from the dry Owens Lake bed and other naturally dry soil surfaces in the valley. Additional chemical tracer measurements will provide evidence of turbulent mixing (cf. Section 2.2). We propose to measure CO, ozone, water vapor, CO<sub>2</sub> and CH<sub>4</sub> on board the HIAPER. The information provided by these tracer measurements will be enhanced with the information from an upward looking lidar onboard the mid-altitude aircraft (BAe146). All aircraft will be equipped with dropsonde systems. Curtains of dropsonde releases for obtaining velocity and thermodynamic data in the air volume below flight tracks are planned along high-altitude cross-mountain and mountain-parallel flight tracks. Generic vertically stacked cross-mountain flight tracks at a range of possible flight track altitudes are shown in Figure 19. The flight design strategy will build on the experience gained in the recent Mesoscale Alpine Programme (MAP) experiment, and will include repeated passes along a selected small number of flight tracks. All research aircraft flights will be coordinated with the operation of ground-based fixed and mobile instrumentation.

Lidars represent a core component of the overall pursuit of the rotor coupled system scientific objectives, since they will routinely scan the atmospheric volume from the surface to many kilometers aloft in both the along- and cross-valley directions. Lidars will provide visualization of rotor and other local flow/shear instability phenomena (cf. Figure 7), aerosol

transport, the relationship between the height of the boundary layer and the aerosol depth, 3-D velocity and rotor characterization, and vertical motions within the valley atmosphere. On the other hand, a scanning K-band radar represents a key instrument for documenting dynamics and microphysics within the rotor and wave clouds.

Aerosol lidars, including the Raman-shifted Eye-safe Aerosol Lidar (REAL; Mayor and Spuler 2004; Spuler and Mayor 2005), which resolves aerosol-based structures at 3.5 m resolution over a 5-10 km range (possibly higher depending on aerosol concentration and extinction), will be deployed to measure the temporal and spatial structure of phenomena over the ground station networks and in the vicinity of the aircraft tracks, and to discern the detailed, diurnally-evolving rotor structures that are a key component of the wave/rotor hypotheses of T-REX. Similarly, but providing crucial velocity information at larger scales, a Doppler lidar has proven to be an effective tool for studying flows in mountainous and other complex terrain, including mountain waves and windstorms (e.g., Neiman et al. 1988, Banta et al. 1990; Clark et al. 1994, 2000; Flamant et al. 2002; Weissmann et al. 2004). Such lidar systems have been built with maximum ranges of 5 to 20 km and range resolutions from 30 to 300 m. They are thus ideally suited to study flows and flow variability in a valley that is ~20 km across, such as Owens Valley. Other characteristics of two such systems can be found in Post and Cupp (1990) and Grund et al. (2001). Doppler lidar systems, such as 2  $\mu\text{m}$  lidars, offer high range resolution and high velocity measurement accuracy. It is anticipated that all these systems should be operating at close to their optimum, because of the dryness of the air and significant lofting of dust by the winds in this region, producing an especially high aerosol loading.

Several Doppler lidar groups will be proposing to participate in T-REX, raising the likelihood of dual or even multiple Doppler lidar coverage. Multiple-Doppler analysis techniques have been well established for Doppler radar. The availability of dual- or multiple-Doppler lidar measurements would provide unparalleled opportunity for scientific advancement, particularly in the assessment of the 3-D structure, and our ability to numerically model (and verify) the rotor coupled system evolution. The dual Doppler coverage allows the computation of all three components of velocity over two 3-D volumes or 'lobes', oriented perpendicular to the baseline connecting the instruments (Figure 20). This computation can be done at spatial resolutions comparable to the resolution of individual lidars (less than 100 m), and at time intervals of a few minutes between successive volumes. A limitation of the dual Doppler analysis is that the vertical velocity calculation requires a boundary condition, which may be difficult to specify reliably in the complex terrain of Owens Valley. This limitation would be relaxed if more than two lidars were deployed. Additional Doppler lidars, of course, would also extend the lidar coverage within the valley, allowing the along-valley variability of the flows to be documented. The significance for the verification of theoretical and numerical modeling studies of being able to provide accurate values of traditionally hard-to-measure vertical component of velocity, along with the horizontal wind components at fine spatial resolution over a 3-D domain, cannot be overstated.

The ground station networks, including dense networks of automatic weather stations and microbarographs, will be used to monitor boundary-layer separation at the surface as well as rotor and wave-induced flows within the valley and on the adjoining mountain slopes. As the experience from Phase I shows, only the strongest rotor cases are likely to be documented by the ground station wind measurements. However, with measurements of surface pressure



gradients, it should be possible to capture a pressure signal at the surface from a rotor aloft, and determine whether this signal is present before the boundary layer separates, and thus tell whether the boundary layer controls the rotor. Part of the answer on the origin and nature of the presumed Type II rotors, will come from observing how the rotor behavior changes under different boundary-layer conditions. Probably the most important amongst these conditions is the surface heat flux, to be measured in detail at flux towers but also measured using flux-gradient assumptions at many of the AWS sites.

In addition to providing wind profiles to characterize the atmospheric state during and between wave/rotor events, the ISS wind profilers will collect high-resolution measurements of Doppler spectral moments. As a continuation of work begun during the Phase I SOP, during which vertical motions in mountain waves were unambiguously observed with profilers (cf. Figure 15), the vertical velocity and spectral width of wind profiler Doppler spectra will be examined for signatures of mountain waves, rotors, and the related turbulence. Special wind profiler observations will be provided by the NCAR Multiple Antenna profiler (MAPR), an advanced boundary layer wind profiler capable of making wind measurements on time scales as short as a few minutes (Cohn et al. 2001). Such fast wind measurement capability is ideal for capturing rapid evolution of waves, and especially rotors. MAPR can also be run in RIM (Range IMaging) mode, a frequency hopping technique, to improve the range resolution of the profiler down to around 20 meters (Palmer et al. 1999). With the presence of both fixed and mobile wind profilers, the vertical velocity and spectral width fields will be examined both along and across the valley axis. Together with the spatial coverage from scanning lidars, the special wind profiler modes will be used to probe within the greater rotor structure.

The effect of changes in the upstream conditions on the formation of waves and rotors will rely on rawinsondes launched at frequent intervals during IOPs from special fixed and mobile platforms in the Central Valley of California, and from the existing network of continuously operating radar wind profilers (RWP) and Radio Acoustic Sounding Systems (RASS). The RWP provide continuous soundings of wind speeds and directions through a depth of ~3 km, while the RASS can provide soundings of virtual temperature through depths of ~1 km. Additionally, dropsondes will provide upwind temperature, wind and humidity soundings that can identify and monitor the mountaintop-level capping inversion layer upwind of the Sierra Nevada and the blocked flow layer below.

## *(2) Transitions from undisturbed to strongly perturbed conditions*

A ground-based observing strategy, based primarily on observations from the continuously operating fixed networks of remote and *in situ* sensors similar to that presented above, will be used to document the boundary-layer structure and its evolution in Owens Valley in the absence of waves and rotors.

The structure and evolution of lee-side boundary layers in Owens Valley will be monitored continuously with networks of instrument systems including automatic weather stations, Doppler sodars, Radio Acoustic Sounding Systems (RASS), and Integrated Surface Flux Facilities (ISFF) (heavily instrumented tall towers) (cf. Figure 18). In addition to these, surface-based microbarographs and cross-barrier lines of temperature sensors will be used to monitor the cross-mountain pressure gradients and cross-valley airmass contrasts. These latter

instrument systems will also be able to monitor the diurnal evolution of the upstream boundary layer structure. A tethered lifting system will be used to directly observe winds, atmospheric stability, and small-scale turbulence within the lower levels of the valley atmosphere (Figure 21; Balsley et al. 1998, Frehlich et al. 2004). Doppler lidars will provide critical information on the structure of the various flows in the valley down to fine scales, as they have in many previous field experiments (Post and Neff 1986; Banta et al. 1996, 1997, 1999, 2004; Darby et al. 1999; Levinson and Banta 1995; McKendry et al. 1997, 1998; Flamant et al. 2002; Drobinski et al. 2001, 2003a,b; Weissmann et al. 2004). The structure of the boundary layer during the rotor onset phase will be monitored with four Doppler sodars.

In order to characterize the heterogeneity of surface/boundary layer, the existing Phase I surface meteorological tower array will be enhanced. The proposed tall towers, heavily instrumented with sonic anemometers, thermocouples, and a full suite of surface energy balance equipment, including very high-rate (100 Hz) momentum flux measuring devices very close to the surface, will provide unprecedented data on the evolution of temperature, humidity, and momentum flux divergence during wave/rotor and non-wave/rotor days. These tall flux towers, along with the existing network of surface towers, and other smaller flux towers will help to identify physical limitations of high-resolution numerical modeling studies within the T-REX program.

With these instruments, uniquely comprehensive observations will be made of diurnal wind fields in the valley, flow channeling, stable boundary layer evolution including cold pools and their destruction by growing convective boundary layers, turbulent erosion, mass removal or buildup by slope flows, large-scale disturbances to local wind fields, and near-surface and boundary-layer fluxes of heat, momentum and moisture. The continuously operating networks of meteorological sensors will also allow investigation of transitions between non-rotor and rotor conditions. Special instrument systems such as dual Doppler lidars, wind profilers, and rawinsondes may be used also to supplement the continuously operating networks during special boundary layer IOPs.

### *(3) Summary of observational requirements*

In summary, the NSF Lower Atmospheric Observing Facilities that will be requested for T-REX are listed in Table 4. A number of T-REX scientists plan to propose to NSF or other domestic and foreign agencies to bring additional facilities to T-REX. The participation of these instrument platforms in T-REX will enhance and expand our observing capabilities. All instrumentation platforms and special instruments to be requested for T-REX are listed in the Appendix starting on page 35. Figures 16 to 20 illustrate the project area and the proposed instrumentation.

## **3.3 Real-Time Numerical Modeling Support**

A dedicated real-time numerical modeling effort in support of T-REX field operations is an integral part of the T-REX experiment design. We expect to have forecasts from several models available in real-time, with products specifically designed to aid in planning and execution of field operations.

Our numerical forecasting plans include special high-resolution real-time COAMPS simulations at a horizontal resolution of at least 3 km in the innermost domain covering Owens Valley. The Weather Research Forecasting model Development Testbed Center (WRF DTC) has also been approached, and T-REX is currently under consideration by the WRF DTC as one of their future real-time testbed projects. The involvement of the WRF DTC in the T-REX effort would provide real-time high-resolution WRF forecasts over the western United States. For forecasting and nowcasting of mountain waves and turbulence, the Mountain Wave Forecasting Model (MWFM) as well as 3DVOM wave forecasting model (Vosper 2003) are expected to be adapted for T-REX needs and run daily to make forecasts available to aid in flight planning and execution for optimal sampling of mountain wave structure, rotors, instability dynamics, and turbulence occurrence by research aircraft. Other model products that would be made available during the T-REX field campaign include clear air turbulence (CAT) algorithms and mountain-wave indicators derived from the ECMWF forecasts, expected to be available at T719 resolution by the spring of 2006.

#### **4. Project Management Structure**

Participants in this project include investigators from a large number of US universities and agencies, the National Center for Atmospheric Research, and several European universities and research institutes (Table 1). The Scientific Steering Committee (SSC; Table 5), comprised of key principal investigators directly involved in the program, is responsible for the overall scientific guidance of the project. The T-REX Project Office, a joint venture between the Desert Research Institute and the UCAR Joint Office for Science Support (JOSS), has been formed to carry out the organizational and coordination tasks for this project.

#### **5. Data Management Plan**

The development and maintenance of a comprehensive and accurate data archive is a critical step in meeting the science objectives of T-REX. A major objective of a comprehensive T-REX data management strategy will be to make as complete a dataset as possible available to the community as soon as possible following the field phase. Oversight of T-REX data management will come from the T-REX SSC in collaboration with the T-REX Project Office. JOSS has been approached by the T-REX SSC to provide assistance with these activities.

JOSS proposes to support the project in the planning and implementation of a comprehensive data management strategy by developing consistent data format and documentation guidelines, policies and protocols to maximize data exchange and access; support to field operations by implementing a JOSS Field Catalog customized for T-REX needs; collaboration in implementing a T-REX data submission and archival process; providing specialized supporting operational data collection and processing; and implementing a comprehensive archive architecture using the JOSS data management system to meet project needs.

Investigators participating in the project are expected to follow project data policies and procedures. These will be consistent with NSF guidelines and assure timely access to the dataset by all project participants and the general scientific community. A T-REX Data Management Plan will be prepared prior to the start of the field phase to guide data management support.

## 6. Project Location and Operations

T-REX is proposed for early spring of 2006. The project will be based in Owens Valley in California; a site chosen because of its unique combination of terrain features and atmospheric conditions that leads to the common occurrence of the famous Sierra Wave and attendant rotors, but also of pronounced cold pools, flow channeling, and thermally-driven flows. Early spring was selected based on climatological studies of mountain wave occurrence in the Sierra Nevada as well as experience of soaring pilots and previous field campaigns in Owens Valley, which indicate that early spring is the optimal time for the wave activity in the southern Sierra Nevada.

We are proposing a two-month field campaign, from 1 March to 30 April 2006. This two-month period in early spring is expected to be sufficiently long for a number of wave and rotor events to occur, but also to provide sufficient time in between individual rotor events to accomplish all of the scientific objectives described in Section 2. All ground-based systems are expected to be in place by the beginning of the project, which climatologically is a preferred time for the documentation of the non-wave-related boundary-layer phenomena.

Two T-REX aircraft, the University of Wyoming King Air and UK BAe146, will be based at the same airport, in the vicinity of the project location. Bishop Airport, a former Army Air Corps airfield and currently a general aviation airport in the largest town at the northern end of Owens Valley, is a prime candidate for an aircraft base of operation. Steps have already been taken to secure needed hangar and office space at this airport. The third aircraft, the NSF/NCAR HIAPER, will operate out of its base at the Jefferson County Airport in Broomfield, Colorado. HIAPER would fly to Owens Valley only for individual IOPs. The expected flight time to Owens Valley is about 2 hours for this aircraft. Some supporting atmospheric chemistry measurements will be conducted during these ferry segments. Possible landing and refueling of this aircraft at the T-REX aircraft base of operation is under active consideration for longer IOPs.

A T-REX Operations Center is also likely to be set up at the Bishop Airport. The Center will provide real time flight coordination to all research aircraft and ground-based observing systems utilizing the Real-Time Display and Coordination Center (RDCC). Other capabilities will include real-time data displays, weather forecasting, Internet access, analysis space, and meeting space. We expect that JOSS will lead in establishing the Operations Center and provide staff experienced in directing and coordinating operations. For weather forecasting, in addition to our planned real-time numerical modeling effort, we plan to work with National Weather Service regional forecasters who have already expressed interest in participating in this effort.

A site survey to select final instrument locations, aircraft operations base, and the Operations Center location will be conducted by a team comprised of T-REX SSC, principal instrumentation investigators, and JOSS staff. JOSS staff will work also with principal investigators to develop a mission planning process and will help design an integrated aircraft observing program. They will also assist in preparations for project forecasting support (cf. Section 3.3), in the development of an overall communications plan, and in the preparation of a T-REX Operations Plan to guide field activities. A valuable real-time information management system will be provided utilizing the JOSS Field Catalog.

## REFERENCES

- Armi, L., 1986: The hydraulics of two flowing layers with different densities, *J. Fluid Mech.*, **163**, 27-58.
- Balsley, B. B., M. L. Jensen, and R. Frehlich, 1998: The use of state-of-the-art kites for profiling the lower atmosphere, *Bound. Layer Meteor.*, **87**, 1-25.
- Banta, R. M., 1986: Daytime boundary-layer evolution over mountainous terrain. Part II: Numerical studies of upslope flow duration. *Mon. Wea. Rev.*, **114**, 1112-1130.
- Banta, R. M., and W. R. Cotton, 1981: An analysis of the structure of local wind systems in a broad mountain basin. *J. Appl. Meteor.*, **20**, 1255-1266.
- Banta, R. M., and P. T. Gannon, 1995: Influence of soil moisture on simulations of katabatic flow. *Theor. Appl. Climatology*, **52**, 85-94.
- Banta, R. M., L. D. Olivier, and J. M. Intrieri, 1990: Doppler lidar observations of the 9 January 1989 severe downslope windstorm in Boulder, Colorado. *Preprints, 5<sup>th</sup> Conf. on Mountain Meteorology*, Boulder CO, Amer. Meteor. Soc., 68-69.
- Banta, R. M., L. D. Olivier, P. H. Gudiksen, and R. Lange, 1996: Implications of small-scale flow features to modeling dispersion over complex terrain. *J. Appl. Meteor.*, **35**, 330-342.
- Banta, R. M., L. S. Darby, P. Kaufmann, D. H. Levinson, and C.-J. Zhu, 1999: Wind flow patterns in the Grand Canyon as revealed by Doppler lidar. *J. Appl. Meteor.*, **38**, 1069-1083.
- Banta, R. M., L. S. Darby, J. D. Fast, B. D. Orr, J. Pinto, W. J. Shaw, and C. D. Whiteman, 2004: Nocturnal low-level jet in a mountain basin complex. I: Evolution and implications to other flow features. *J. Appl. Meteor.*, in press.
- Banta, R. M., P. B. Shepson, J. W. Bottenheim, K. G. Anlauf, H. A. Wiebe, A. J. Gallant, T. Biesenthal, L. D. Olivier, C.-J. Zhu, I. G. McKendry, and D. G. Steyn, 1997: Nocturnal cleansing flows in a tributary valley. *Atmos. Environ.*, **31**, 2147-2162.
- Bright, D. R., and S. L. Mullen, 2002: The sensitivity of the numerical simulation of the southwest monsoon boundary layer to the choice of PB turbulence parameterization in MM5. *Wea. Forecast.*, **17**, 99-114.
- Broutman, D., J. W. Rottman, and S. D. Eckermann, 2003: A simplified Fourier method for nonhydrostatic mountain waves. *J. Atmos. Sci.*, **60**, 2686-2696.
- Businger, J. A., 1973: Turbulent transfer in the atmospheric surface layer. in D. H. Haugen (ed.), *Workshop on Micrometeorology*, American Meteor. Soc., Boston, MA, pp. 67-100.
- Businger, J. A., J. C. Wyngaard, Y. Izumi, and E. F. Bradley, 1971: Flux-profile relationships in the atmospheric surface layer. *J. Atmos. Sci.*, **28**, 181-189.
- Cahill, T. A., T. E. Gill, D. A. Gillette, E. A. Gearhart, J. S. Reid, and M.-L. Yau, 1994, Generation, characterization, and transport of Owens (Dry) Lake dusts, Final Report: California Air Resources Board, Sacramento, Contract No. A132-105, 166 p.

- Carney, T. Q., A. J. Bedard, J. M. Brown, M. J. Kraus, J. McGinley, and T. A. Lindholm, 1995: *Hazardous Mountain Winds and Their Visual Indicators*. Department of Commerce/NOAA, 80pp.
- Carson, D. J., and P. J. R. Richards, 1978: Modelling surface turbulent fluxes in stable conditions. *Bound.-Layer Meteor.*, **14**, 68-81.
- Chen F., T. T. Warner, and K. Manning, 2001: Sensitivity of orographic moist convection to landscape variability: A study of the Buffalo Creek, Colorado, flash flood case of 1996. *J. Atmos. Sci.*, **58**, 3204-3223.
- Chen, Y., F. L. Ludwig, F. L., & R. L. Street, 2004a: Stably-stratified flows near a notched, transverse ridge across the Salt Lake Valley. *J. Appl. Meteor.*, **43**, 1308-1328.
- Chen, Y., R. L., Street, and F. L. Ludwig, 2004b: On rotors, internal waves and hydraulic jumps in simulated stably-stratified flows in Utah's Salt Lake valley, *11th Conference on Mountain Meteorology*, AMS, June 2004, Bartlett, NH, P1.2, 5 pages.
- Cho, J. Y. N. et al., 1999: Observations of convective and dynamical instabilities in tropopause folds and their contribution to stratosphere-troposphere exchange. *J. Geophys. Res.*, **104**, 21, 549-21.
- Chow, F. K., 2004: Subfilter-scale turbulence modeling for large-eddy simulation of the atmospheric boundary layer over complex terrain. Ph.D. Dissertation, Stanford University.
- Chow, F. K., R. L. Street, M. Xue, and J. H. Ferziger, 2005: Explicit filtering and reconstruction turbulence modeling for large-eddy simulation of neutral boundary layer flow, *J. Atmos. Sci.*, in press.
- Clark. T. L., 1977: A small-scale dynamic model using a terrain-following coordinate transformation. *J. Comput. Phys.*, **24**, 186-215.
- Clark, T. L., W. D. Hall, and R. M. Banta, 1994: Two- and three-dimensional simulations of the 9 January 1989 windstorm: Comparison with observations. *J. Atmos. Sci.*, **51**, 2317-2343.
- Clark, T. L., W. D. Hall, R. M. Kerr, D. Middleton, L. Radke, F. M. Ralph, P. J. Nieman, and D. Levinson, 2000: Origins of aircraft-damaging clear-air turbulence during the 9 December 1992 Colorado downslope windstorm: Numerical simulations and comparison with observations. *J. Atmos. Sci.*, **57**, 1105-1131.
- Cohn, S. A., W. O. J. Brown, C. L. Martin, M. S. Susedik, G. Maclean, and D. B. Parsons, 2001: Clear air boundary layer spaced antenna wind measurement with the Multiple Antenna Profiler (MAPR), *Ann. Geophys.*, **19**, 845-854.
- Corby, G. A., 1954: The airflow over mountains - a review of the state of current knowledge. *Quart. J. Roy. Meteor. Soc.*, **80**, 491-521.
- Cullen, M. J. P., 1993: The unified forecast/climate model. *Meteorol. Mag.*, **122**, 81-94.
- Darby, L. S., W. D. Neff, and R. M. Banta, 1999: Multiscale analysis of a meso- $\alpha$  frontal passage in the complex terrain of the Colorado Front Range. *Mon Wea. Rev.*, **127**, 2062-2081.

- De Wekker, S. F. J., D. G. Steyn, and S. Nyeki, 2004: A comparison of aerosol layer- and convective boundary layer structure over a mountain range during STAAARTE '97. *Bound.-Layer Meteor.*, **113**, 249-271.
- Derbyshire, S.H., 1999: Boundary-layer decoupling over cold surfaces as a physical boundary instability. *Bound.-Layer Meteor.*, **90**, 297-325.
- Doran J. C., J. D. Fast, and J. Horel, 2002: The VTMX 2000 campaign. *Bull. Amer. Meteor. Soc.*, **83**, 537-551.
- Doyle, J. D., D. R. Durran, C. Chen, B. A. Colle, M. Georgelin, V. Grubišić, W. R. Hsu, C. Y. Huang, D. Landau, Y. L. Lin, G. S. Poulos, W. Y. Sun, D. B. Weber, M. G. Wurtele, M. Xue, 2000: An intercomparison of model predicted wave breaking for the 11 January 1972 Boulder windstorm. *Mon. Wea. Rev.*, **128**, 901-914.
- Doyle, J. D., and D. R. Durran, 2002: The dynamics of mountain-wave induced rotors. *J. Atmos. Sci.*, **59**, 186-201.
- Doyle, J. D., and D. R. Durran, 2004a: Recent developments in the theory of atmospheric rotors. *Bull. Amer. Meteor. Soc.*, **85**, 337-342.
- Doyle, J. D., and D. R. Durran, 2004b: On the structural characteristics and dynamics of sub-rotors. *11<sup>th</sup> Conference on Mountain Meteorology*, AMS, June 2004, Bartlett, NH.
- Doyle, J. D., and R. B. Smith, 2003: Mountain waves over the Hohe Tauern. *Quart. J. Roy. Meteor. Soc.*, **129**, 799-823.
- Drobinski P., A. M. Dabas., C. Haerberli, P. H. Flamant, 2001: On the small-scale dynamics of flow splitting in the Rhine Valley during a shallow foehn event. *Bound.-Layer Meteor.*, **99**, 277-296.
- Drobinski P., C. Haerberli, E. Richard, M. Lothon, A. M. Dabas, P. H. Flamant, M. Furger, R. Steinacker, 2003a: Scale interaction processes during MAP-IOP 12 south foehn event in the Rhine Valley. *Quart. J. Roy. Meteorol. Soc.*, **129**, 729-754.
- Drobinski P., A. M. Dabas, C. Haerberli, P. H. Flamant, 2003b: Statistical characterization of the flow structure in the Rhine Valley. *Bound.-Layer Meteor.*, **106**, 483-505.
- Durran, D. R., 1986: Another look at downslope windstorms. Part I: The development of analogs to supercritical flow in an infinitely deep, continuously stratified fluid. *J. Atmos. Sci.*, **43**, 2527-2543.
- Eckermann, S. D., J. Ma, and D. Broutman, 2004: The NRL Mountain Wave Forecast Model (MWFm). *50<sup>th</sup> Anniv. Symposium on Operational Numerical Weather Prediction*, AMS, College Park, MD, June 2004.
- Eckermann, S. D. and P. Preusse, 1999: Global measurements of stratospheric mountain waves from space, *Science*, **286**, 1534-1537.
- Ehernberger, L. J., 1987: High-altitude turbulence for supersonic cruise vehicles, *NASA Tech. Memo. 88285*, 15 pp.
- Elliott, W. P., 1964: The height variation of vertical heat flux near the ground. *Quart. J. Roy. Meteor. Soc.*, **90**, 260-265.

- Flamant, C., P. Drobinsky, L. Nance, R. Banta, L. Darby, J. Dusek, M. Hardesty, J. Pelon, and E. Richard, 2002: Gap flow in an Alpine valley during a shallow south foehn event: Observations, numerical simulations and hydraulic analog. *Quart. J. Roy. Meteor. Soc.*, **128**, 1173-1210.
- Frehlich, R. G., Y. Meillier, M. L. Jensen, B. B. Balsley: 2004: A statistical description of small-scale turbulence in the low-level nocturnal jet, *J. Atmos. Sci.*, **61**, 1079-1085.
- Fritts, D. C., and M. J. Alexander, 2003: Gravity wave dynamics and effects in the middle atmosphere. *Rev. Geophys.*, **41(1)**, 1003, doi:10.1029/2001RG000106.
- Fujita, T. T., 1989: The Teton-Yellowstone tornado of 21 July 1987. *Mon. Wea. Rev.*, **117**, 1913-1940.
- Gheusi, F. J., J. Stein, and O. Eiff, 2000: A numerical study of three dimensional orographic gravity wave breaking observed in a hydraulic tank. *J. Fluid Mech.*, **410**, 67-99.
- Gill, T. E., and D. A. Gillette, 1991: Owens Lake: A natural laboratory for aridification, playa desiccation and desert dust. *Geological Society of America Abstracts with Programs*, **23**, no. 5, p. 462.
- Goerss, J. S. 2000: Tropical cyclone track forecasts using an ensemble of dynamical models. *Mon. Wea. Rev.*, **128**, 1187-1193.
- Gross, G., and, F. Wippermann, 1987: Channeling and countercurrent in the upper Rhine Valley: Numerical simulations. *J. Climate Appl. Meteor.*, **26**, 1293-1304.
- Grubišić, V., 2005: Sierra Rotors Project IOP 8: High-resolution numerical simulations. In preparation.
- Grubišić, V., and S. Cardon, 2002: Climatology of the Sierra Nevada mountain-wave clouds. *Preprints, 10th Conf. Mountain Meteorology*, AMS, June 2002, Park City, UT, 392-393.
- Grubišić, V., and J. M. Lewis, 2004: Sierra Wave Project revisited: 50 years later. *Bull. Amer. Meteor. Soc.*, **85**, 1127-1142.
- Grubišić, V., and J. P. Kuettner, 2004: Sierra rotors and the Terrain-induced Rotor Experiment (T-REX). *11th Conf. on Mountain Meteorology and Annual Mesoscale Alpine Program (MAP) Meeting*, AMS, June 2004, Bartlett, NH, Online preprint [http://ams.confex.com/ams/11Mountain/techprogram/paper\\_77384.htm](http://ams.confex.com/ams/11Mountain/techprogram/paper_77384.htm)
- Grubišić, V., and S. A. Cohn, 2004: Sierra Rotors Project: Preliminary findings. *11th Conf. on Mountain Meteorology and the Annual Mesoscale Alpine Programme (MAP) Meeting*. AMS, June 2004, Bartlett, NH, Online preprint [http://ams.confex.com/ams/11Mountain/techprogram/paper\\_77364.htm](http://ams.confex.com/ams/11Mountain/techprogram/paper_77364.htm)
- Grubišić, V., and B. Billings, 2005: The Sierra Nevada mountain wave climatology. In preparation.
- Grund, C. J., R. M. Banta, J. L. George, J. N. Howell, M. J. Post, R. A. Richter, and A. M. Weickmann, 2001: High-resolution Doppler lidar for boundary-layer and cloud research. *J. Atmos. Ocean. Technol.*, **18**, 376-393.



- Hertenstein, R. F., and J. P. Kuettner, 2005: Rotor types associated with steep lee topography: Influence of the wind profile. *Tellus A*. In press.
- Hodur, R. M., 1997: The Naval Research Laboratory's Coupled Ocean/Atmosphere Mesoscale Prediction System (COAMPS). *Mon. Wea. Rev.*, **111**, 1414-1430.
- Holmboe, J., and H. Klieforth, 1957: Investigation of mountain lee waves and the airflow over the Sierra Nevada. Final Report. Department of Meteorology, UCLA, Contract AF 19(604)-728, 283pp.
- Holton, J. R., P. H. Haynes, M. E. McIntyre, A. R. Douglas, R. B. Rood, and L. Pfister, 1995: Stratosphere-troposphere exchange. *Rev. Geophys.*, **33**, 403-439.
- Hopkins, R.H., 1994: Anchorage windstorm of 1 December 1992. *Wea. and Forecast.*, **4**, 469-478.
- Jiang, Q., J. D. Doyle, and R. B. Smith, 2005: Interaction between trapped waves and boundary layers. Submitted to *J. Atmos. Sci.*
- Kaplan, M. L., et al. 2004a: Characterizing the severe turbulence environments associated with commercial aviation accidents. A 44 case study synoptic observational analyses. In press. *Meteor. Atmos. Phys.*
- Kaplan, M. L., et al., 2004b: Characterizing the severe turbulence environments associated with commercial aviation accidents. Hydrostatic mesoscale numerical simulations of supergradient wind flow and ageostrophic along-stream frontogenesis. In press. *Meteor. Atmos. Phys.*
- Kaplan, M. L. et al., 2004c: Characterizing the severe turbulence environments associated with commercial aviation accidents. A Real-Time Turbulence Model (RTTM) Designed for the Operational Prediction of Hazardous Aviation Turbulence Environments. Submitted *Meteor. Atmos. Phys.*
- Kim, Y.-J., S. D. Eckermann, and H.-Y. Chun, 2003: An overview of the past, present, and future of gravity-wave drag parameterization for numerical climate and weather prediction models. *Atmos.-Ocean*, **41**, 65-98.
- King, C. W., 1997: A climatology of thermally forced circulations in oppositely oriented airsheds along the continental divide in Colorado. Technical Memorandum ERL ETL-283, National Oceanic and Atmospheric Administration, Environmental Research Laboratories, Boulder, CO, 152pp.
- King M. D., S. Platnick, P. Yang, G. T. Arnold, M. A. Gray, J. C. Riedi, S. A. Ackerman, and K.-N. Liou, 2004: Remote sensing of liquid water and ice cloud optical thickness and effective radius in the Arctic: Application of airborne multispectral MAS data. *J. Atmos. Ocean. Tech.*, **21**, 857-875.
- Kondo, J., O. Kanechika., and N. Yasuda, 1978: Heat and momentum transfers under strong stability in the atmospheric surface layer. *J. Atmos. Sci.*, **35**, 1012-1021.
- Koschmieder, H., 1920: Zwei bemerkenswerte Beispiele horizontaler Wolkenschlaeuche. *Beitr. Phys. fr. Atm.*, **9**, 176-180.

- Kossmann, M., U. Corsmeier, S. F. J. De Wekker, F. Fiedler, R. Vögtlin, N. Kalthoff, H. Güsten, and B. Neininger, 1999: Observations of handover processes between the atmospheric boundary layer and the free troposphere over mountainous terrain. *Contrib. Atmos. Phys.*, **72**, 329-350.
- Kuettner, J. P., 1938: Moazagotl und Foehnwelle. *Beitr. Phys. Frie Atmos.*, **25**, 79-114.
- Kuettner, J. P., 1939: Zur Entstehung der Foehnwelle. *Beitr. Phys. Frei Atmos.*, **25**, 251-299.
- Kuettner, J., 1959: The rotor flow in the lee of mountains. Geophysics Research Directorate (GRD) Research Notes 6, AFCRC-TN-58-626, Air Force Cambridge Research Center, USA, 20 pp.
- Kuettner, J., and R. F. Hertenstein, 2002: Observations of mountain-induced rotors and related hypotheses: A review. *Preprints, 10th Conf. Mountain Meteorology*, AMS, June 2002, Park City, UT, 326-329.
- Langland, R., R. L. Elsberry, and R. M. Errico, 1996: Adjoint sensitivity of an idealized extratropical cyclone with moist physical processes. *Quart. J. Roy. Meteor. Soc.*, **122**, 1891-1920.
- Lester, P. F., and W. A. Fingerhut, 1974: Lower turbulent zones associated with mountain lee waves. *J. Appl. Meteor.*, **13**, 54-61.
- Levinson, D. H., and R. M. Banta, 1995: Observations of a terrain-forced mesoscale vortex and canyon drainage flows along the Front Range of the Colorado Rockies. *Mon. Wea. Rev.*, **123**, 2029-2050.
- Lilly, D. K., and W. Toutenhoofd, 1969: The Colorado Lee Wave program. *Clear Air Turbulence and Its Detection*. Plenum Press, 232-245.
- Louis, J. F., 1979: A parametric model of vertical eddy fluxes in the atmosphere. *Bound.-Layer Meteor.*, **17**, 187-202.
- Lyra, G., 1943: Theorie der stationären Leewellenströmung in freier Atmosphäre. *Z. angew. Math. Mech.*, **23**, 1-28.
- Mahrt, L., 1998a: Stratified atmospheric boundary layers, *Bound.-Layer Meteor.*, **905**, 375-396.
- Mahrt, L., 1998b: Flux sampling errors for aircraft and towers. *J. Atmos. Ocean. Tech.*, **15**, 416-429.
- Mahrt, L., and D. Vickers, 2003: Formulation of Turbulent Fluxes in the Stable Boundary Layer. *J. Atmos. Sci.*, **60**, 2538-2548.
- Mayor, S. D. and S. M. Spuler, 2004: Raman-shifted eye-safe aerosol lidar, *Appl. Optics*, **43**, 3915-3924.
- Mayr, G. J., J. Vergeiner, and A. Gohm, 2002: An automobile platform for the measurement of foehn and gap flows. *J. Atmos. Oceanic. Techn.*, **19**, 1545-1556.
- McKendry, I. G., D. G. Steyn, R. M. Banta, W. Strapp, K. Anlauf, and J. L. Pottier, 1998: Daytime photochemical pollutant transport over a tributary valley lake in southwestern British Columbia. *J. Appl. Meteor.*, **37**, 393-404.

- McKendry, I. G., D. G. Steyn, J. Lundgren, R. M. Hoff, J. W. Strapp, K. G. Anlauf, F. Froude, B. A. Martin, R. M. Banta, and L. D. Olivier, 1997: Elevated ozone layers and vertical downmixing over the Lower Fraser Valley, B.C. *Atmos. Environ.*, **31**, 2135–2146.
- Mass, C. F., D. Ovens, K. Westrick, B. A. Colle, 2002: Does Increasing Horizontal Resolution Produce More Skillful Forecasts? *Bull. Amer. Meteor. Soc.*, **83**, 407–430.
- Mobbs, S. D., S. B. Vosper, P. F. Sheridan, R. Cardoso, R. R. Burton, S. J. Arnold, M. K. Hill, V. Horlacher, and A. M. Gadian, 2004: Observations of downslope winds and rotors in the Falkland Islands. Submitted to *Quart. J. Roy. Meteor. Soc.*
- Nastrom, G. D., and D. C. Fritts, 1992: Sources of mesoscale variability of gravity waves, I: Topographic excitation, *J. Atmos. Sci.*, **49**, 101–110.
- Neiman, P. J., R. M. Hardesty, M. A. Shapiro, and R. E. Cupp, 1988: Doppler lidar observations of a downslope windstorm. *Mon. Wea. Rev.*, **116**, 2265–2275.
- Oke, T. R., 1970: Turbulent transport near the ground in stable conditions. *J. Appl. Meteor.*, **9**, 778–786.
- Ólafsson, H. and P. Bougeault, 1997: The effect of rotation and surface friction on orographic drag. *J. Atmos. Sci.*, **54**, 193–210.
- Palmer, R. D., T. Y. Yu, and P. B. Chilson, 1999: Range imaging using frequency diversity, *Radio Sci.*, **34**, 1485–1496.
- Pavelin, E., J. A. Whiteway, R. Busen, and J. Hacker, 2002: Airborne observations of turbulence, mixing, and gravity waves in the tropopause region. *J. Geophys. Res.*, **107**(D10), 10.1029/2001JD000775.
- Pawlak, G., and L. Armi, 2000: Mixing and entrainment in developing stratified currents. *J. Fluid Mech.*, **424**, 45–73.
- Pielke, R. A., et al., 1992: A comprehensive meteorological modeling system RAMS. *Meteor. Atmos. Phys.*, **49**, 69–91.
- Post, M. J., and W. D. Neff, 1986: Doppler lidar measurements of winds in a narrow mountain valley. *Bull. Amer. Meteor. Soc.*, **67**, 274–281.
- Post, M. J. and R. E. Cupp, 1990: Optimizing a pulsed Doppler lidar. *Appl. Opt.*, **29**, 4145–4158.
- Poulos, G. S., 1996: The interaction of mountain waves and katabatic flows. Dissertation [Available from Colorado State University, Department of Atmospheric Sciences, Fort Collins, Colorado, 80523], 399 pp.
- Poulos, G. S., J. E. Bossert, R. A. Pielke and T. B. McKee, 2000: The interaction of katabatic flow and mountain waves I: Observations and idealized simulations. *J. Atmos. Sci.*, **57**, 1919–1936.
- Poulos, G. S., W. Blumen, D. C. Fritts, J. K. Lundquist, J. Sun, S. P. Burns, C. Nappo, R. Banta, R. Newsome, J. Cuxart, E. Terradellas, B. Balsley, and M. Jensen, 2002: CASES-99: A comprehensive investigation of the stable nocturnal boundary layer. *Bull. Amer. Meteor. Soc.*, **83**, 555–581.

- Poulos, G. S., and S. P. Burns, 2003: An evaluation of bulk Ri-based surface layer flux formulae for stable and very stable conditions with intermittent turbulence. *J. Atmos. Sci.*, **60**, 2523-2537. (*William Blumen Memorial and CASES-99 Special Issue*).
- Powell, D. and H. Klieforth, 1991: Chapter 1, Weather and Climate, *The Natural History of the White-Inyo Range*, C. Hall, Ed., University of California Press, Berkeley, pp 3-26.
- Queney, P., G. A. Corby, N. Gerbier, H. Koschmieder, and J. Zierep, 1960: *The Airflow Over Mountains*. WMO Technical Note No. 34. World Meteorological Organization, Geneva, Switzerland.
- Raloff, J., 2001: Dust, Part 2: Ill winds. *Science News*, **160**, no. 14, p. 218.
- Ralph, F. M., P. J. Neiman, T. L. Keller, D. Levinson, and L. Fedor, 1997: Observations, simulations, and analysis of nonstationary trapped lee waves. *J. Atmos. Sci.*, **54**, 1308-1333.
- Reheis, M. C., 1997: Dust deposition downwind of Owens (dry) Lake, 1991-1994: Preliminary findings: *J. Geophys. Res.*, **102**(D22), 25999-26008, 10.1029/97JD01967.
- Reiter, E. R., and H. P. Foltz, 1967: The prediction of clear air turbulence over mountainous terrain. *J. Appl. Meteor.*, **6**, 549-556.
- Richard, E., P. Mascart, and E. C. Nickerson, 1989: The role of surface friction in downslope winstorms. *J. Appl. Meteor.*, **28**, 241-251.
- Schär, C., D. Leuenberger, O. Fuhrer, D. Lüthi, and C. Girard, 2002: A new terrain-following vertical coordinate formulation for atmospheric prediction models. *Mon. Wea. Rev.*, **130**, 2459-2480.
- Scorer, R. S., 1949: Theory of waves in the lee of mountains. *Quart. J. Roy. Meteor. Soc.*, **75**, 41-46.
- Scorer, R. S., and H. Klieforth, 1959: Theory of mountain waves of large amplitude. *Quart. J. Roy. Meteor. Soc.*, **85**, 131-143.
- Smith, R. B., 1989: Hydrostatic Airflow over Mountains. *Adv. Geophysics*, **31**, 1-41.
- Smith, R. B, S. T. Skubis, J. D. Doyle, A. Broad, C. Kiemle and H. Volkert, 2002. Mountain waves over Mt. Blanc: Influence of a stagnant boundary layer. *J. Atmos. Sci.*, **59**, 2073-2092.
- Smith, R.B., Q. Jiang, and J.D. Doyle, 2005: A theory of gravity wave absorption by boundary layers. Submitted to *J. Atmos. Sci.*
- Smolarkiewicz, P. K., and L. G. Margolin, 1997: On forward in-time differencing for fluids: An Eulerian/semi-Lagrangian non-hydrostatic model for stratified flows. *Atmos.-Ocean*, **35** (special issue), 127-152.
- Spuler, S. M. and S. D. Mayor, 2005: Scanning eye-safe aerosol backscatter lidar at 1.54 microns, Submitted to *J. of Atmos. and Oceanic Tech.*
- Stefanutti, L., L. Sokolov, S. Balestri, A. R. MacKenzie, and V. Khattatov, 1999: The M-55 Geophysica as a platform for the Airborne Polar Experiment, *J. Atmos. Oceanic Technol.*, **16**, 1303-1312.

- Stewart, J. Q., C. D. Whiteman, W. J. Steenburgh, and X. Bian, 2002: A climatological study of thermally driven wind systems of the US Intermountain West. *Bull. Amer. Meteor. Soc.*, **83**, 699-708.
- Stohl, A. et al., 2003: Stratosphere-troposphere exchange: A review, and what we have learned from STACCATO, *J. Geophys. Res.*, **108**(D12), 8516, doi:10.1029/2002JD002490.
- Van de Wiel, B. J. H., R. J. Ronda, A. F. Moene, H. A. R. de Bruin, and A. A. M. Holtslag, 2002a. Intermittent turbulence and oscillations in the stable boundary layer over land. Part I: A bulk model. *J. Atmos. Sci.*, **59**, 942-958.
- Van de Wiel, B. J. H., A. F. Moene, R. J. Ronda, H. A. R. de Bruin, and A. A. M. Holtslag, 2002b, Intermittent turbulence and oscillations in the stable boundary layer over land. Part II: A system dynamics approach, *J. Atmos. Sci.*, **59**, 2567-2581.
- Van de Wiel, B. J. H., A. F. Moene, O. K. Hartogensis, H. A. R. de Bruin, and A. A. M. Holtslag, 2003: Intermittent turbulence and oscillations in the stable boundary layer over land. Part III: A classification for observations during CASES-99, *J. Atmos. Sci.*, **60**, 2509-2522.
- Vosper, S. B., 2003: Development and testing of a high-resolution mountain-wave forecasting system. *Meteorol. App.*, **10**, 75-86.
- Vosper, S. B., 2004: Inversion effects on mountain lee waves. *Quart. J. Roy. Meteor. Soc.*, **130**, 1723-1748.
- Webb, E. K., 1970: Profile relationships: The log-linear range and extension to strong stability. *Quart. J. Roy. Meteor. Soc.*, **96**, 67-90.
- Weissmann, M. D., G. J. Mayr, R. M. Banta, and A. Gohm, 2004: Observations of the temporal evolution and structure of gap flow in the Wipp Valley on 2 and 3 October 1999. *Mon. Wea. Rev.*, **132**, 2684-2697.
- Whiteman, C. D., 1982: Breakup of temperature inversions in deep mountain valleys: Part I. Observations. *J. Appl. Meteor.*, **21**, 270-289.
- Whiteman, C. D., 1990: Observations of Thermally Developed Wind Systems in Mountainous Terrain. Chapter 2 in Atmospheric Processes Over Complex Terrain, (W. Blumen, Ed.), *Meteorological Monographs*, **23**, no. 45., Amer. Meteor. Soc., Boston, Massachusetts, 5-42.
- Whiteman, C. D., 2000: *Mountain Meteorology: Fundamentals and Applications*. Oxford University Press, New York, 355 pp.
- Whiteman, C. D., and J. C. Doran, 1993: The relationship between overlying synoptic-scale flows and winds within a valley. *J. Appl. Meteor.*, **32**, 1669-1682.
- Whiteman, C. D., S. Zhong, and X. Bian, 1999a: Wintertime boundary layer structure in the Grand Canyon. *J. Appl. Meteor.*, **38**, 1084-1102.
- Whiteman, C. D., X. Bian, and S. Zhong, 1999b: Wintertime Surface Wind Patterns in the Colorado River Valley. *J. Appl. Meteor.*, **38**, 1118-1130.
- Xiao, X., D. S. McRae, and H. A. Hassan, 2005: Dynamically Resolved Simulation of Atmospheric Features and Turbulence, AIAA Paper 2005-0625, January 2005.

## APPENDIX: MAJOR FACILITIES AND INSTRUMENTATION

The following is a listing of all major facilities and instrumentation that will be requested for T-REX.

### Satellite

*GOES*: Special floater sections of the GOES satellite will be requested for coverage during the field project period. High-resolution 1 km scenes will be examined for signatures of the Sierra waves, and foehn windows.

### Aircraft

*NSF/NCAR HIAPER Gulfstream V*: The development of HIAPER (the High-performance Instrumented Airborne Platform for Environmental Research), the new high-altitude NSF research platform, is scheduled for completion in June 2005, and in late December 2005 this new research platform is expected to become available for the start of research mission support. It is expected that by summer 2005, this aircraft will be equipped with standard instrumentation, including sensors for atmospheric state parameters (temperature, pressure, humidity), air motion (wind), and a dropsonde system. Three groups of instruments will be requested for this experiment. These are 1) remote sensors, 2) *in situ* chemical tracers, and 3) microphysics probes. They are the following:

- 1) Two remote sensors: SABL (or a new eye-safe lidar) and MTP
- 2) Four *in situ* chemical tracers instruments: CO (RAF/Teresa Campos), H<sub>2</sub>O (RAF/Teresa Campos) and Ozone (instrument will be provided by NCAR, PI Andy Weinheimer). We will also request the HIAPER QCL (CO<sub>2</sub>/CH<sub>4</sub>) instrument (PI Steve Wofsy) if available at the time of the experiment.
- 3) Microphysics probes: Cloud and Aerosol Spectrometer Probe (CAPS, PI Andy Heymsfield), Forward Scattering Sepctrometer Probe (FSSP, RAF instrument), Cloud particle Imager (CPI, RAF), and Video Ice Particle Imager (PI Andy Heymsfield).

*Wyoming King Air 200T*: The University of Wyoming King Air 200T (N2UW) is a double-engine turbo-prop with a wide range of sensors for measurements of atmospheric state parameters, air motion, cloud properties, and video photography. Special instrumentation that will be requested for this aircraft is the dropsonde system in support of the dynamical objectives of the experiment.

*UK BAe146*: The United Kingdom Natural Environmental Research Council BAe146 aircraft has been requested by the UK scientists for participation in T-REX. This aircraft is jointly managed by the UK Met Office and the consortium of UK universities. The University of Leeds

group currently has 25 hours of flying time funded. The additional number of flying hours to be contributed by the UK Met Office is not yet confirmed but it is expected that *in total* this aircraft would be available for a period of around 6 weeks with 6 to 10 research flights conducted during this time. Several other currently planned UK NERC and Met Office initiatives are likely to add more hours and extend the time for which this aircraft will be available. Besides the standard instrumentation packages for measurement of atmospheric state parameters (temperature, humidity, etc.) and air motion, this aircraft will be equipped with an aerosol lidar configured in a downward pointing mode used to measure dust and/or water vapor signature due to rotors. The dropsonde system will also be available. For cloud microphysical measurements this aircraft will be equipped with special instrumentation such as the mark 2 Small Ice Detector (SID-2), a wider range of aerosol physical and chemical measurements and vertical velocity measurements of greater absolute accuracy (within a few 10s of  $\text{cm s}^{-1}$ ).

## **Ground-based remote sensors**

### ***Lidars***

*NOAA MINI-MOPA:* NOAA 10  $\mu\text{m}$  (eye-safe)  $\text{CO}_2$  Doppler lidar with air-tight laser that can operate on  $\text{CO}_2^{18}$  isotope. The expected range of this lidar is 15 km in aerosol-laden air with the variable range resolution of 75-200 m, and a velocity measurement precision of  $25 \text{ cm s}^{-1}$ .

*DLR Doppler Lidar:* Coherent 2  $\mu\text{m}$  pulsed Doppler lidar. The maximum range is about 5-10 km with range resolution of 25-100 m. The accuracy of the velocity measurements is around  $0.1 \text{ m s}^{-1}$ . The vertical scan range is  $20^\circ$  or greater with the scan duration of 11 s. If pointing vertically, this lidar can measure vertical velocities.

*ASU Doppler Lidar:* Coherent 2- $\mu\text{m}$  Doppler lidar with 500 Hz pulse repetition frequency (PRF). A typical maximum range is 5-10 km. The finest range resolution is 50 – 100 m. This is a commercial lidar built by Coherent Technologies, Inc.

*NASA GSFC GLOW:* Goddard Lidar Observatory for Wind is a mobile Doppler lidar system based on double edge direct detection technology. It consists of a molecular system at  $0.355 \mu\text{m}$  and an aerosol system at  $1.064 \mu\text{m}$ .

*NASA GSFC SRL:* This Scanning Raman Lidar makes use of Raman scattering in the atmosphere to measure various atmospheric properties, such as water vapor mixing ratio, aerosol scattering ratio and extinction, and liquid water mixing ratio.

*NCAR REAL:* Operating at 1.54  $\mu\text{m}$ , this Raman-shifted Eye-safe Aerosol Lidar (REAL) resolves aerosol-based structures at 3.5 m resolution over a 5-10 km range (depending on extinction). REAL is expected to aid in determining the sources of turbulent bursts that are likely to be observed on the tall tower network, and in documenting subrotor structures and aerosol layer heights (<http://www.lidar.ucar.edu>).

*NRL Aerosol Lidar:* The lidar operates at 1.5  $\mu\text{m}$  at 50 Hz and the range resolution is 1.5 m up to a 20 km range depending on conditions. An earlier version of this lidar was used to measure boundary layer eddy structure, turbulence and aerosol structure sizes. The lidar has a two axis scanning system, which can be used dynamically to track and measure the evolution of individual aerosol structures. We expect the NRL Lidar to be useful in depicting the characteristics of the turbulent structures within the rotor including documentation of subrotor structures.

### ***Other remote sensors***

*NCAR ISS:* The Integrated Sounding Systems consisting of four separate subsystems: a 915 MHz Doppler clear-air wind profiling radar, radio acoustic sounding system (RASS), enhanced surface observing station, and balloon borne radiosonde sounding system. Three of these systems will be deployed in T-REX: ISS with Multiple Antenna Profiler (MAPR), Mobile ISS (MISS), and a regular fixed ISS. The first two of these systems were also deployed in the Phase I field effort in spring 2004. The ISS with MAPR is an advanced boundary layer wind profiler capable of making wind measurements on time scales as short as a few minutes. MAPR can also be run in RIM (Range IMaging) mode, a frequency hopping technique, to improve the range resolution of the profiler down to around 20 meters or better. The MAPR ISS will also deploy a sodar to obtain additional wind measurements in the lowest 300 meters.

*Sodars:* Four (4) additional sodars will be deployed in Owens Valley during T-REX. Three of these sodars will be provided by the University of Leeds, one by the University of Houston. These systems are expected to give wind and temperature profiles at 15-minute intervals up to 700-1000 m in wind speeds less than about 20  $\text{m s}^{-1}$ .

*Yale K-band radar:* One or two low-power vertically-pointing 24 GHz METEK radars will be deployed near the Sierra ridge crest to monitor the precipitation intensity and the location of the foehn wall. This instrument has a one-minute time resolution. It sees to an altitude 3 km above the station with a 105 meter vertical resolution. This FM/CW system can measure the speed and density of falling hydrometeors, at light precipitation rates.

### **Other ground-based instrumentation**

*DRI surface network:* This network of automatic weather stations with telemetry was the core of instrumentation in the Phase I field effort. The network consists of sixteen (16) instrumented



10-m meteorological towers, and a base station located in Independence. The 900-MHz spread-spectrum radio-communication is used to relay 30-second data on 10-m winds, and 2-m temperature, relative humidity and pressure between individual stations and the base station. From the base station the data are sent via Internet to the data repository at DRI. This network has been continuously reporting surface meteorological data since February 2004. The data is available online in near-real time at <http://www.wrcc.dri.edu/trex>.

*University of Leeds surface network:* Network of 16 automatic weather stations without telemetry and up to 16 additional microbarographs recording 30-second data will be installed in Owens Valley, extending the existing DRI network coverage within the valley and up the mountain slopes, all the way to the crest of the Sierra at the Kearsarge Pass. Parts of this network are planned to be in place as early as spring 2005.

*Soil Probes:* Up to 30 soil moisture and soil temperature probes will be provided by Stanford University and deployed throughout the valley to measure the spatial variability in these surface properties. The probes will be co-located with other surface stations where possible, so that air measurements and fluxes will be available. The soil sensors can be co-located with the University of Leeds automatic weather stations, which will extend along the eastern slope of the Sierras, as well as with the DRI surface network located lower in the valley.

*University of Utah HOBOS:* Solar-shielded continuously operated temperature data loggers will be used to collect data at 5-minute intervals. Approximately fifty (50) of these temperature data loggers will be installed in Owens Valley in mountain-parallel and mountain-perpendicular lines to extend the existing and planned surface networks.

*NCAR Mobile GLASS (MGAOS):* The mobile GLASS rawinsonde system, completely self-contained in a camper shell that can be carried by a full-size pickup truck, includes equipment to conduct atmospheric soundings and make supporting surface meteorological observations.

*NCAR ISFF:* The Integrated Surface Flux Facility will be deployed with three 32-m-tall heavily instrumented towers capable of measuring flux profiles and turbulence intermittency with very high rate ( $> 100$  Hz). Along with standard instrumentation, each tower will be outfitted with a suite of sonic anemometers, thermocouples and thin-film anemometers below 5 m AGL. In order to assess the spatial heterogeneity of intermittent turbulence, one tower will be placed in a 'central' location with other two towers placed orthogonally (on the along-valley axis and cross-valley axis) a few to many hundreds of meters away from the central tower. The ISFF also includes surface flux measurement capabilities, which will be used to measure soil moisture, soil temperature, soil heat fluxes, and radiation fluxes at these locations.

*Flux Towers:* Two 15-m flux tower systems recording raw turbulence data (including temperature perturbations) using sonic anemometers at two heights (University of Leeds). These

towers will have surface energy budget measurement capability (net radiation, soil heat flux and humidity fluxes). One 10-m flux tower will also be deployed to collect complete surface energy budget measurements (University of Houston).

*University of Colorado Tethered Lifting System (TLS):* The TLS uses hi-tech kites or aerodynamic blimps to carry one to five sensors (suspended well below the tether) for high-resolution velocity, temperature, and turbulence measurements. The fundamental advantage of TLS *in situ* sampling lies with its high-resolution capability (sample rates of >200 Hz combined with the slow track of the sensors through the atmosphere). TLS data on wind speed/direction, temperature and turbulence can provide critical information for calibrating remote sensing instruments such as lidars, FMCW radars and boundary-layer wind profilers by providing vertically-structured mean flows with vertical resolutions < 1m. The University of Colorado TLS technique also employs a manned Powered Parachute (PPC) that can fly to similar altitudes and carry ~60 kg payloads (CO<sub>2</sub>, ozone, particle counters, temperature chains, turbulence sensors, etc.). The PPC is not tethered, and can make along-valley and cross-valley transects at relatively slow speeds between surface and ~3km.

*University of Innsbruck Instrumented Car:* A mobile weather station with temperature, humidity, pressure, and wind (2-D sonic anemometer) sensors mounted on a passenger car (Mayr et al. 2002) will be used with GPS location information to make cross-valley and along-valley traverses during selected wave and non-wave events.

*Yale Time-Lapse Video Camera System:* One or two S-video time lapse systems will be installed to monitor wave clouds, rotor clouds, convection, dust and the foehn wall during daylight hours. The system operates unattended, taking a moderate resolution image every 4 seconds. To avoid sun glare, the cameras will be positioned to look NW, N, or NE. One such system was deployed successfully in Phase I.

## **LIST OF TABLES**

Table 1: Participating scientists and organizations

Table 2: T-REX scientific objectives

Table 3: Research aircraft and their capabilities

Table 4: NSF Lower Atmospheric Observing Facilities Pool Request

Table 5: T-REX Scientific Steering Committee

## LIST OF FIGURES

- Figure 1: Shaded relief topographic map of the central and southern Sierra Nevada (left panel) and Owens Valley (right panel). The north-south elongated Owens Valley lies in between the Sierra Nevada and the White-Inyo mountain ranges, which define its west and east walls, respectively. The yellow dotted line in the right panel shows the position of the cross-valley measurement transect through Independence, California and the location of the dry bed of Owens Lake (provided by D. Durran).
- Figure 2: Number of days with observed mountain wave clouds. Top panel: From Küttner (1939), based on total of 212 observations of wave clouds from Germany (“Moazagotl”), England (“Helm-bar”), and other countries (“andere Gelände”). Bottom panel: Results of a recent cloud satellite climatology of mountain waves in the Sierra Nevada showing number of days with lee wave and Sierra wave clouds in the southern portion of the Sierra Nevada in two consecutive years in the late 1990s (from Grubišić and Billings 2005).
- Figure 3: Illustrations of the two-layer structure of the rotor flow. Top: Flow over the White Mountains of New Hampshire as viewed from the top of Mt. Washington. Wind direction is from the left (Photo: R. Lavoie). Bottom: Flow over mountains east of San Diego taken while soaring in the mountain wave aloft. Clouds mark the top of the coastal marine layer. Wind direction from the right. (Photo: L. Armi).
- Figure 4: Top: Type I rotor cloud near Boulder, Colorado (Photo: R. Hertenstein, 23 December 2003). Left: Type II rotor cloud viewed from 9,800 m looking south along Owens Valley with the Sierra Nevada to the right. Wind direction from the right (Photo: T. Henderson).
- Figure 5: Streamlines illustrating differences between rotor types in an idealized 2-D simulation. Type I rotor simulation shown in (a) was obtained with  $10^{-2} \text{ s}^{-1}$  horizontal wind shear in the initial upstream inversion, and Type II shown in (b) with no shear in the initial upstream inversion (from Hertenstein and Kuettner 2005.)
- Figure 6: Wind vectors and y-component of vorticity in an (a) x-y plane at 1700 m and (b) x-z cross-section along segment AB through a numerically simulated rotor ( $\Delta x=67 \text{ m}$ ). Flow is from the left. Considerable variability in the structure along the mean rotor axis (y-direction) is evident in (a). The main rotor lies underneath the crest of the first lee wave, as illustrated in (b), and is clearly a rather chaotic circulation with many fine-scale features (“subrotors”). The highest vorticity is found where the rising vortex sheet has rolled-up into a subrotor on the upstream side of the wave. Strong downslope flow is evident in the lower left part of the figure (from Doyle and Durran 2004b).
- Figure 7: Low-level airflow during 9 January 1989 severe downslope windstorm over Boulder, Colorado, as measured by NOAA’s Scanning Doppler Lidar. Wind vectors within the cone over the lidar position may be spurious. Note a near-surface flow reversal

indicating rotor development at  $x > 4$  km, and sub-rotor vortices aloft at  $x = 6$  km and  $x = 11-12$  km (from Banta et al. 1990).

Figure 8: Vertical cross section of simulated streamlines and cross-mountain wind component (color scale,  $\text{m s}^{-1}$ ) oriented across the Sierra Range using COAMPS valid at 00 UTC 20 November 1996 (24-h simulation time). The  $20 \text{ m}^2 \text{ s}^{-2}$  turbulence kinetic energy contour is shown by the bold black contour. The simulation used five nested grids with the innermost mesh ( $\Delta x=333$  m) shown here. A complex low-level rotor circulation is apparent in Owens Valley along with reversed flow aloft associated with wave breaking near 10 km ASL above the Sierra crest. A commercial airline encountered severe turbulence that resulted in an injury near this time and above Bishop, CA at  $\sim 9$  km asl (provided by J. Doyle).

Figure 9: Average temperature and circulation over the DRI ground station network area in Owens Valley during March 2004 during Sierra Rotors Project. Black dots indicate AWS locations. Top row: Temperature in degrees C. Bottom row: Wind vectors. At 02 PST, a cold pool (top left) with northerly wind in the valley and downslope flow on the western slope (bottom left). At 15 PST, the highest temperatures are found at the valley floor (top right), with the southerly and upslope winds over the network area (bottom right). (Provided by V. Grubišić from the SRP data).

Figure 10: Top: Schematic depiction of the phase transition process in a wave cloud (A. Heymsfield). Bottom: Multilayer structure of wave clouds in the lee of the Sierra Nevada. View southward along Owens Valley from about 9 km on 1 May 1955 during the Sierra Wave Project. The rotor (roll) clouds are at about 4.5 km, whereas the highest wave cloud is near 12 km. The original photo has been rotated around its vertical axis to show wind from the left (Photo: T. Henderson).

Figure 11: Penetration of a severe rotor by an instrumented B-29 aircraft at 500 hPa level, showing 20 positive and negative vertical gusts reaching  $\pm 20 \text{ m s}^{-1}$  over less than a minute (from the Sierra Wave Project, Holmboe and Klieforth 1957).

Figure 12: Base map of the Sierra Rotors Project (SRP) location and instrumentation. Red symbols show the location of the Sierra Rotors Project instrumentation. Shown is also a preexisting network of the Great Basin Unified Air Pollution Control District (GBUSAPCD) automatic weather stations clustered around the dry Owens Lake bed (From Grubišić and Kuettner 2004).

Figure 13: Left: NCEP GFS model prediction of wind, geopotential height, and vorticity at 500 hPa for 00 UTC 26 March 2004 during SRP IOP 8 showing a classical prefrontal situation conducive of wave generation in Owens Valley. Bottom left: GOES10 visible satellite image from 01 UTC March 26 (17 PST March 25). Bottom right: A view from the ground of the rotor and wave clouds around 01 UTC March 26. Dust, lofted from the dry Owens Lake bed by strong westerly winds, is visible in the far south. View southeast from west of Independence (from Grubišić and Cohn 2004; Photo: V. Grubišić).

Figure 14: Evolution of the mountain wave and rotor during 25-26 March 2004 in SRP IOP 8). Times shown are: March 25, 20 UTC (left), March 26 at 01 UTC (middle) and March 26 at 03 UTC (right). UTC = PST + 8 hours. Top row: Model simulated potential temperature and the westerly wind component in the east-west vertical cross-section through Independence. The cross-section is from the innermost domain (horizontal resolution of 333 m) of a COAMPS simulation with five nested grids. Middle row: Objective analysis of the 10-m wind data measured by the ground network at those times. Bottom: Terrain of Owens Valley surrounding the DRI ground network. The westerly wind component ( $\text{m s}^{-1}$ ) is shown on top of the terrain surface. A ground footprint of a rotor is seen at 19 LST, with a large-amplitude wave and the rotor over Owens Valley, and the downslope flow of  $15\text{-}20 \text{ m s}^{-1}$  over the western slope (provided by V. Grubišić).

Figure 15: Mountain wave as seen by the ISS/MAPR wind profiler (right) and a sounding from Owens Valley from 12 UTC 26 March 2004 obtained during SRP IOP 8 (cf. Figure 14). Note strong up- (red) and down- (blue) drafts documented by the wind profiler. A radiosonde, launched from the ISS/MAPR site, was pulled down about 500 meters into dry warm air by the downdraft (provided by S. Cohn).

Figure 16: T-REX flight-plan schematic showing the orientation of possible cross-mountain flight tracks over the Sierra Nevada and the White-Inyo range. Base map created by the UCAR Joint Office of Scientific Support.

Figure 17: Schematic view of a generic T-REX composite observing system showing major instrumentation in approximate relation to the rotor phenomenon (provided by V. Grubišić and J. Doyle).

Figure 18: Color relief map of the central portion of Owens Valley showing the T-REX field campaign area and the proposed ground-based instrumentation. A GPS sounding site at NAS Lemoore (pink diamond) and the MGLASS location (red star) and are expected to be the same as in the Sierra Rotors Project (cf. Figures 12 and 16). The regular NWS upper-air sounding locations in the surrounding area: Oakland, CA, Vandenberg AFB, CA, and Reno, NV are also shown in Figure 16. (Map: V. Grubišić in collaboration with the UCAR Joint Office of Scientific Support.)

Figure 19: Generic cross-mountain flight tracks with dropsonde releases and the vertical range of all three planned aircraft shown in relation to the terrain, in the vertical cross-section whose base line is indicated with a bold dashed line in Figure 16.

Figure 20: Topographic map of Owens Valley surrounding Independence showing a potential configuration for two Doppler lidars (black circles) sited along a line perpendicular to the ridge and valley axes. Dashed circles represent the area of coverage of individual lidars assuming 12-km range. The union of solid circles (minus their intersection) represents an area of overlap for dual-Doppler velocity calculations, where both lidar beams intersect at an angle between  $30^\circ$  and  $150^\circ$ . The area along the baseline, in between the two lidars, is not available for dual-Doppler wind calculations because the angle between the scan planes is too small to provide two

accurate horizontal wind components. This particular configuration provides an extended dual-Doppler coverage of along-valley flow variability. Lidars could also be oriented so that their baseline is along the axis of the valley, providing extended dual-Doppler coverage in the cross-valley direction. Additionally, three Doppler lidars could be arranged in a triangle configuration, and, if available, quadruple Doppler lidars, in a square or double triangle configuration, extending the coverage in both the along- and cross-valley directions. (Diagram: D. Durran).

Figure 21: High-resolution profiles obtained using the Tethered Lifting System (TLS) in the CASES-99 campaign. Upper panels show profiles of 1 s wind speed (left) and temperature data (right), and the polynomial fitted curves (solid lines). Potential temperature polynomial fit is shown as dashed curve. Lower panels show 20-second smoothed wind direction (left) and 20-second smoothed profile of energy dissipation rate (right). While this figure shows results up to 400 m, the TLS can produce similar results up to ~3 km at roughly hourly intervals. The dark vertical line on the left of each panel illustrates the height of a 55 m instrumented tower for reference (provided by B. Balsely).

**Table 1**  
**Participating Scientists and Organizations**

<b>Name</b>	<b>Affiliation</b>	<b>E-mail Address</b>	<b>Sponsor</b>	<b>NSF funding needed?</b>
Laurence Armi	SCRIPPS	<a href="mailto:larmi@ucsd.edu">larmi@ucsd.edu</a>	NSF	Yes
Ben B. Balsley	CIRES	<a href="mailto:balsley@cires.colorado.edu">balsley@cires.colorado.edu</a>	NSF	Yes
Robert Banta	NOAA/ETL	<a href="mailto:Robert.Banta@noaa.gov">Robert.Banta@noaa.gov</a>	NOAA	Yes
Barbara Brooks	University of Leeds	<a href="mailto:b.j.brooks@leeds.ac.uk">b.j.brooks@leeds.ac.uk</a>	UK NERC	No
Phil Brown	UK Met Office	<a href="mailto:phil.brown@metoffice.com">phil.brown@metoffice.com</a>	UK Met Office	No
William Brown	NCAR/ATD	<a href="mailto:wbrown@ucar.edu">wbrown@ucar.edu</a>	NCAR	No
Ralph Burton	University of Leeds	<a href="mailto:r.r.burton@leeds.ac.uk">r.r.burton@leeds.ac.uk</a>	UK NERC	No
Ronald Calhoun	Arizona State University	<a href="mailto:Ronald.Calhoun@asu.edu">Ronald.Calhoun@asu.edu</a>	NSF	Yes
Teresa Campos	NCAR	<a href="mailto:campos@ucar.edu">campos@ucar.edu</a>	NCAR	No
Tina Katopodes Chow	LLNL	<a href="mailto:katopod@stanford.edu">katopod@stanford.edu</a>	DOE	Yes
Steve Cohn	NCAR/ATD	<a href="mailto:cohn@ucar.edu">cohn@ucar.edu</a>	NCAR	No
Jeff Copeland	NCAR/RAP	<a href="mailto:Copeland@ucar.edu">Copeland@ucar.edu</a>	DHS	No
Larry Cornman	NCAR/RAP	<a href="mailto:cornman@ucar.edu">cornman@ucar.edu</a>	DHS, FAA	No
William R. Cotton	Colorado State University	<a href="mailto:cotton@atmos.colostate.edu">cotton@atmos.colostate.edu</a>	NSF	Yes
Andreas Dörnbrack	DLR	<a href="mailto:andreas.doernbrack@dlr.de">andreas.doernbrack@dlr.de</a>	DLR	No
Belay Demoz	NASA	<a href="mailto:demoz@agnes.gsfc.nasa.gov">demoz@agnes.gsfc.nasa.gov</a>	NASA	No
Stephan DeWecker	NCAR/ASP	<a href="mailto:dewekker@ucar.edu">dewekker@ucar.edu</a>	NCAR	No
James Doyle	NRL	<a href="mailto:doyle@nrlmry.navy.mil">doyle@nrlmry.navy.mil</a>	NRL	No
Stephen Eckermann	NRL	<a href="mailto:eckerman@uap2.nrl.navy.mil">eckerman@uap2.nrl.navy.mil</a>	NRL	No
Rod Frehlich	CIRES & NCAR/RAP	<a href="mailto:frehlich@ucar.edu">frehlich@ucar.edu</a>	NSF	Yes
Dave Fritts	CoRA	<a href="mailto:dave@cora.nwra.com">dave@cora.nwra.com</a>	NSF	Yes
Alexander Gohm	University of Innsbruck	<a href="mailto:alexander.gohm@uibk.ac.at">alexander.gohm@uibk.ac.at</a>	FWF	No
Vanda Grubišić	Desert Research Institute	<a href="mailto:Vanda.Grubisic@dri.edu">Vanda.Grubisic@dri.edu</a>	NSF	Yes



<b>Name</b>	<b>Affiliation</b>	<b>E-mail Address</b>	<b>Sponsor</b>	<b>NSF funding needed?</b>
Patrick Haines	ARL White Sands Missile Range	<a href="mailto:phaines@arl.army.mil">phaines@arl.army.mil</a>	US Army	No
Bill Hall	NCAR	<a href="mailto:hallb@ucar.edu">hallb@ucar.edu</a>	NCAR	No
Hassan A. Hassan	NCSU	<a href="mailto:hassan@eos.ncsu.edu">hassan@eos.ncsu.edu</a>	NSF	Yes
Andrew Heymsfield	NCAR	<a href="mailto:heyms1@ucar.edu">heyms1@ucar.edu</a>	NCAR	No
Rolf Hertenstein	CoRA	<a href="mailto:herten@cora.nwra.com">herten@cora.nwra.com</a>	NSF	Yes
Martin Hill	University of Leeds	<a href="mailto:m.k.hill@leeds.ac.uk">m.k.hill@leeds.ac.uk</a>	UK NERC	No
William Hooper	NRL	<a href="mailto:hooper@ccf.nrl.navy.mil">hooper@ccf.nrl.navy.mil</a>	NRL	No
Janet Intrieri	NOAA/ETL	<a href="mailto:janet.intrieri@noaa.gov">janet.intrieri@noaa.gov</a>	NOAA	Yes
Michael Jensen	CIRES	<a href="mailto:mike@cires.colorado.edu">mike@cires.colorado.edu</a>	NSF	Yes
Qingfang Jiang	UCAR	<a href="mailto:qingfang@ucar.edu">qingfang@ucar.edu</a>	NRL	No
Michael L. Kaplan	NCSU	<a href="mailto:mlkaplan@unity.ncsu.edu">mlkaplan@unity.ncsu.edu</a>	NSF	Yes
Jason Knievel	NCAR/RAP	<a href="mailto:knievel@ucar.edu">knievel@ucar.edu</a>	DHS	No
Joachim Kuettner	NCAR	<a href="mailto:kuettner@ucar.edu">kuettner@ucar.edu</a>	NSF	No
Todd Lane	NCAR	<a href="mailto:lane@ucar.edu">lane@ucar.edu</a>	NCAR	No
Yuh-Lang Lin	NCSU	<a href="mailto:yl_lin@ncsu.edu">yl_lin@ncsu.edu</a>	NSF	Yes
D. Scott McRae	NCSU	<a href="mailto:mrae@eos.ncsu.edu">mrae@eos.ncsu.edu</a>	NSF	Yes
Georg Mayr	University of Innsbruck	<a href="mailto:Georg.Mayr@uibk.ac.at">Georg.Mayr@uibk.ac.at</a>	FWF	No
Shane Mayor	NCAR/ATD	<a href="mailto:shane@mead.atd.ucar.edu">shane@mead.atd.ucar.edu</a>	NCAR	No
John McHugh	University of New Hampshire	<a href="mailto:jpm@cisunix.unh.edu">jpm@cisunix.unh.edu</a>	NSF	Yes
Jim McQuaid	University of Leeds	<a href="mailto:jim@env.leeds.ac.uk">jim@env.leeds.ac.uk</a>	UK NERC	No
Yannick Meillier	CIRES	<a href="mailto:Yannick.Meillier@Colorado.edu">Yannick.Meillier@Colorado.edu</a>	NSF	Yes
Stephen Mobbs	University of Leeds	<a href="mailto:s.d.mobbs@leeds.ac.uk">s.d.mobbs@leeds.ac.uk</a>	UK NERC	No
Laura Pan	NCAR/ACD	<a href="mailto:liwen@ucar.edu">liwen@ucar.edu</a>	NCAR	No
Gregory Poulos	NCAR/ATD	<a href="mailto:gsp@ucar.edu">gsp@ucar.edu</a>	NCAR	No
Stefan Rahm	DLR	<a href="mailto:Stephan.Rahm@dlr.de">Stephan.Rahm@dlr.de</a>	DLR	No
Robert Sharman	NCAR/RAP	<a href="mailto:sharman@ucar.edu">sharman@ucar.edu</a>	DHS, FAA	No

<b>Name</b>	<b>Affiliation</b>	<b>E-mail Address</b>	<b>Sponsor</b>	<b>NSF funding needed?</b>
Ronald B. Smith	Yale University	<a href="mailto:ronald.smith@yale.edu">ronald.smith@yale.edu</a>	NSF	Yes
Robert L. Street	Stanford University	<a href="mailto:street@stanford.edu">street@stanford.edu</a>	NSF	Yes
Simon Vosper	UK Met Office	<a href="mailto:simonv@env.leeds.ac.uk">simonv@env.leeds.ac.uk</a>	UK Met Office	No
Jeff Weil	NCAR/RAP	<a href="mailto:weil@ucar.edu">weil@ucar.edu</a>	DHS	No
Andy Weinheimer	NCAR	<a href="mailto:wein@ucar.edu">wein@ucar.edu</a>	NCAR	No
Martin Weissmann	DLR	<a href="mailto:Martin.Weissmann@dlr.de">Martin.Weissmann@dlr.de</a>	DLR	No
C. David Whiteman	University of Utah	<a href="mailto:whiteman@met.utah.edu">whiteman@met.utah.edu</a>	NSF	Yes
Steve Wofsy	Harvard University	<a href="mailto:wofsy@fas.harvard.edu">wofsy@fas.harvard.edu</a>	NSF	Yes
Xudong Xiao	NCSU	<a href="mailto:xxiao@eos.ncsu.edu">xxiao@eos.ncsu.edu</a>	NSF	Yes
Sharon Zhong	University of Houston	<a href="mailto:szhong@uh.edu">szhong@uh.edu</a>	NSF	Yes

## Table 2

### T-REX Scientific Objectives

To improve the understanding of:

- I) Dynamics and Structure of the Rotor Coupled System**
  - Role of Upstream Flow Properties
  - Wave/Rotor Dynamic Interactions
  - Internal Rotor Structure
  - Rotor/Boundary-Layer Interactions
  - Upper-Level Wave Breaking and Turbulence
  
- II) Complementary Scientific Issues**
  - Stratosphere-Troposphere Exchange
  - Boundary-Layer Structure and Evolution in Absence of Rotors
  - Wave Cloud Phase Transitions and Layering

To achieve improvements in:

- III) Mesoscale and Microscale Modeling**
  - Predictability
  - Physical Parameterizations
  - Representation of Steep Terrain
  - Mesoscale Verification
  
- IV) Prediction**
  - Aviation Hazards
  - Downslope Windstorms
  - Aerosol Transport and Dispersion

**Table 3****Research aircraft and their capabilities**

Research Aircraft	Height Range (kft)	Endurance (h)	Special Instrumentation
HIAPER (NSF/NCAR)	30 – 48	14	aerosol lidar (SABL or an eye-safe lidar), dropsondes, MTP, chemistry
King Air 200T (U Wyoming)	0 – 28	5	dropsondes
BAe146 (UK)	20 – 32	5	aerosol lidar, dropsondes, microphysical probes, chemistry

N.B.: The UK aircraft is already (partly) funded for 50-60 research hours and is reserved for a total of 6 weeks in the field.

**Table 4**

**NSF Lower Atmospheric Observing Facilities Pool Request**

<b>Facility</b>	<b>Request</b>
HAIPER GV	120 hrs including ferry flights
Wyoming King Air	120 hrs plus ferry from/to Laramie, WY
Integrated Sounding Systems (3)	2 month field deployment
Integrated Surface Flux Facility	3 32-m towers, 2 month field deployment
MGAOS	2 month field deployment

## Table 5

### T-REX Scientific Steering Committee

Vanda Grubišić	Desert Research Institute, Reno, Nevada Chair
Joachim Kuettner	National Center for Atmospheric Research, Boulder, Colorado
Robert Banta	NOAA Environmental Research Laboratory, Boulder, Colorado
James Doyle	Naval Research Laboratory, Monterey, California
Stephen Mobbs	University of Leeds, Leeds, UK
Greg Poulos	NCAR Atmospheric Technology Division, Boulder, Colorado
Dave Whiteman	University of Utah, Salt Lake City, Utah
Ronald Smith	Yale University, New Haven, Connecticut Advisor

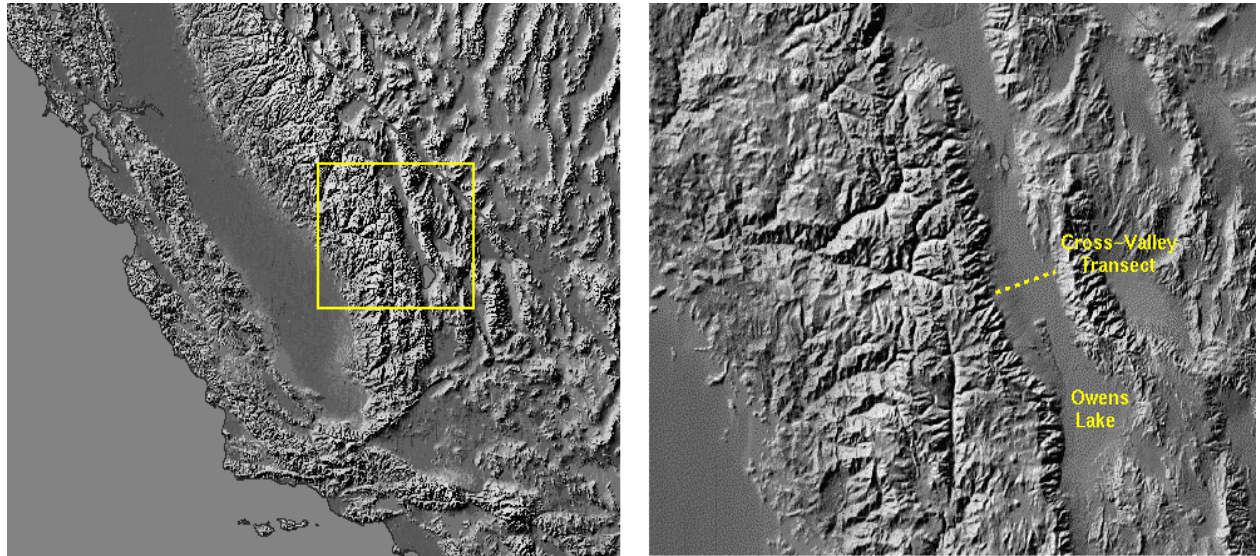


**Figure 1**

Shaded relief topographic map of the central and southern Sierra Nevada (left panel) and Owens Valley (right panel). The north-south elongated Owens Valley lies in between the Sierra Nevada and the White-Inyo mountain ranges, which define its west and east walls, respectively. The yellow dotted line in the right panel shows the position of the cross-valley measurement transect through Independence, California and the location of the dry bed of Owens Lake (provided by D. Durran).

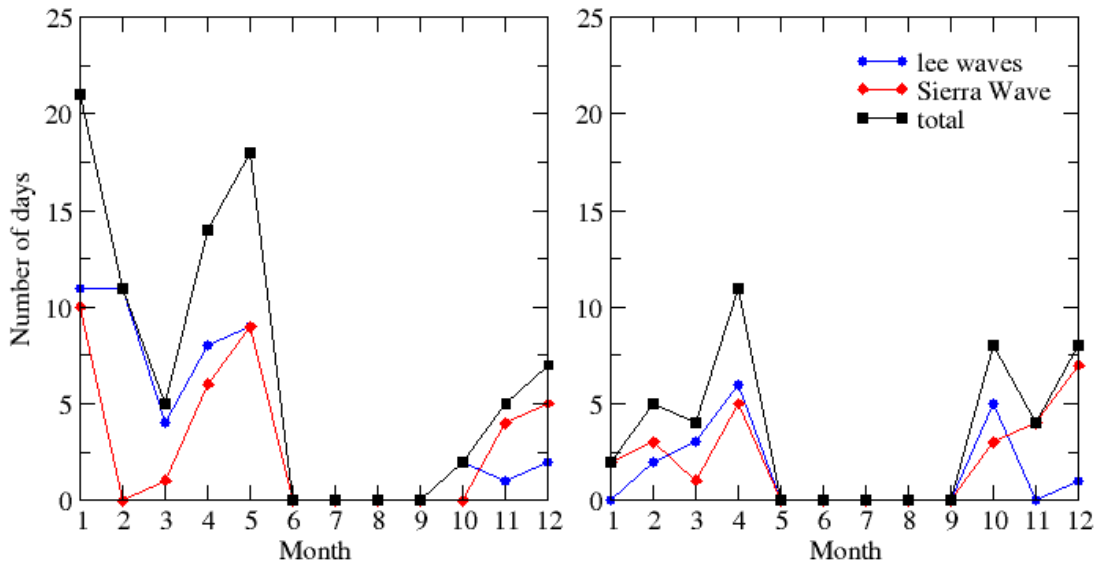
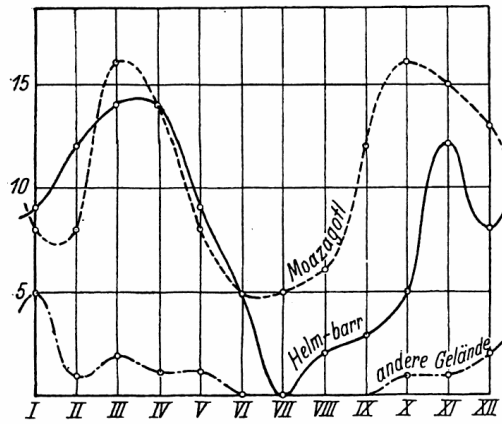


**Figure 2**

Number of days with observed mountain wave clouds. Top panel: From Küttner (1939), based on total of 212 observations of wave clouds from Germany (“Moazagotl”), England (“Helm-bar”), and other countries (“andere Gelände”). Bottom panel: Results of a recent cloud satellite climatology of mountain waves in the Sierra Nevada showing number of days with lee (trapped) wave and Sierra Wave clouds in the southern portion of the Sierra Nevada in two consecutive years in the late 1990s. (from Grubišić and Billings 2005).





**Figure 3**

Illustrations of the two-layer structure of the rotor flow. Top: Flow over the White Mountains of New Hampshire as viewed from the top of Mt. Washington. Wind direction is from the left (Photo: R. Lavoie). Bottom: Flow over mountains east of San Diego taken while soaring in the mountain wave aloft. Clouds mark the top of the coastal marine layer. Wind direction from the right. (Photo: L. Armi).



**Figure 4**

Top: Type I rotor cloud near Boulder, Colorado (Photo: R. Hertenstein, 23 December 2003).  
Left: Type II rotor cloud viewed from 9,800 m looking south along Owens Valley with the Sierra Nevada to the right. Wind direction from the right. (Photo: T. Henderson).

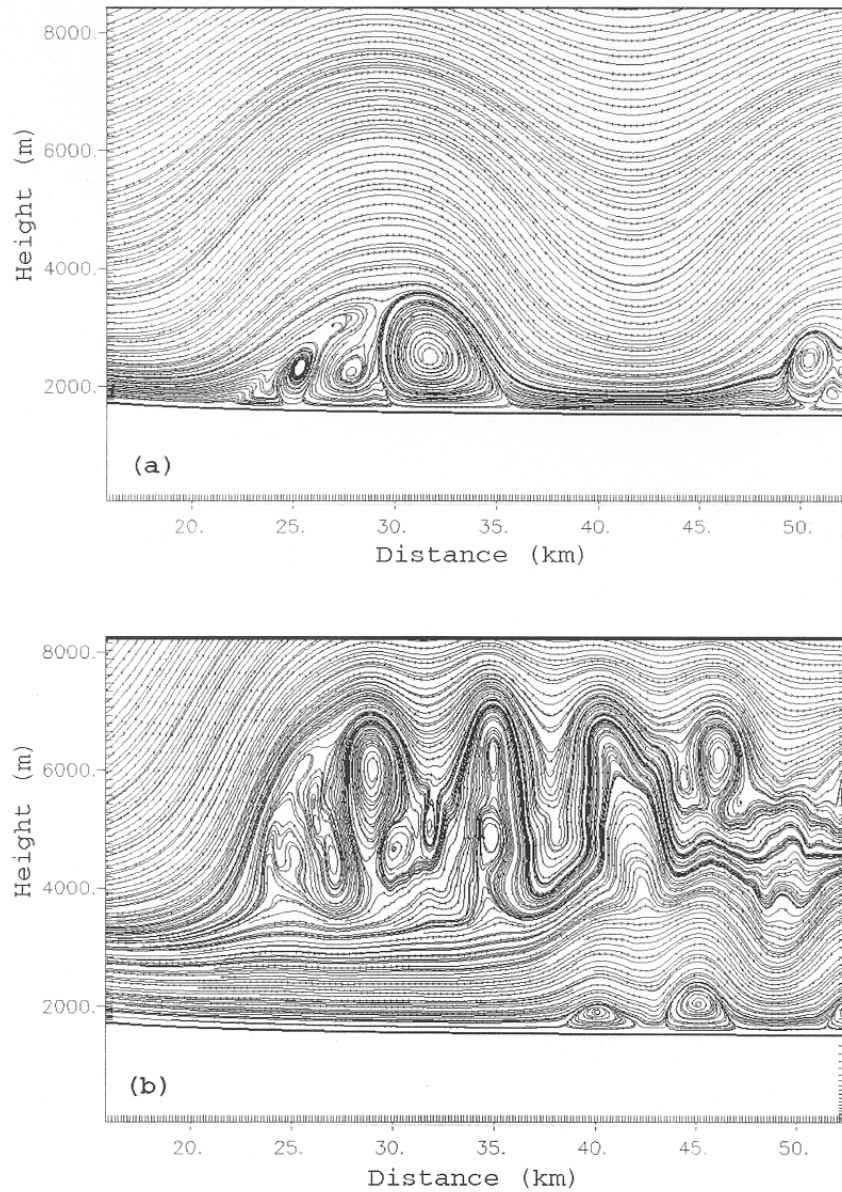


**Figure 5**

Streamlines illustrating differences between rotor types in an idealized 2-D simulation. Type I rotor simulation shown in (a) was obtained with  $10^{-2} \text{ s}^{-1}$  horizontal wind shear in the initial upstream inversion, and Type II shown in (b) with no shear in the initial upstream inversion (from Hertenstein and Kuettnner 2005.)

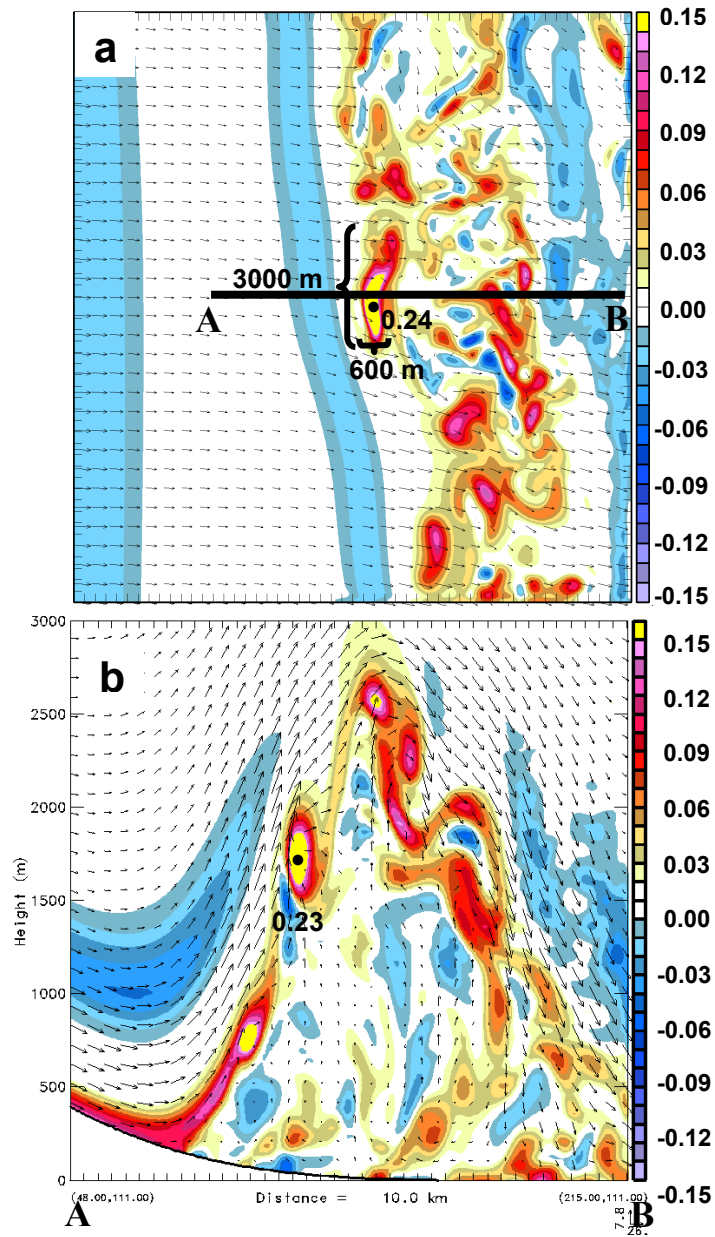


**Figure 6**

Wind vectors and y-component of vorticity in an (a) x-y plane at 1700 m and (b) x-z cross-section along segment AB through a numerically simulated rotor ( $\Delta x=67$  m). Flow is from the left. Considerable variability in the structure along the mean rotor axis (y-direction) is evident in (a). The main rotor lies underneath the crest of the first lee wave, as illustrated in (b), and is clearly a rather chaotic circulation with many fine-scale features (“subrotors”). The highest vorticity is found where the rising vortex sheet has rolled-up into a subrotor on the upstream side of the wave. Strong downslope flow is evident in the lower left part of the figure (from Doyle and Durran 2004b).



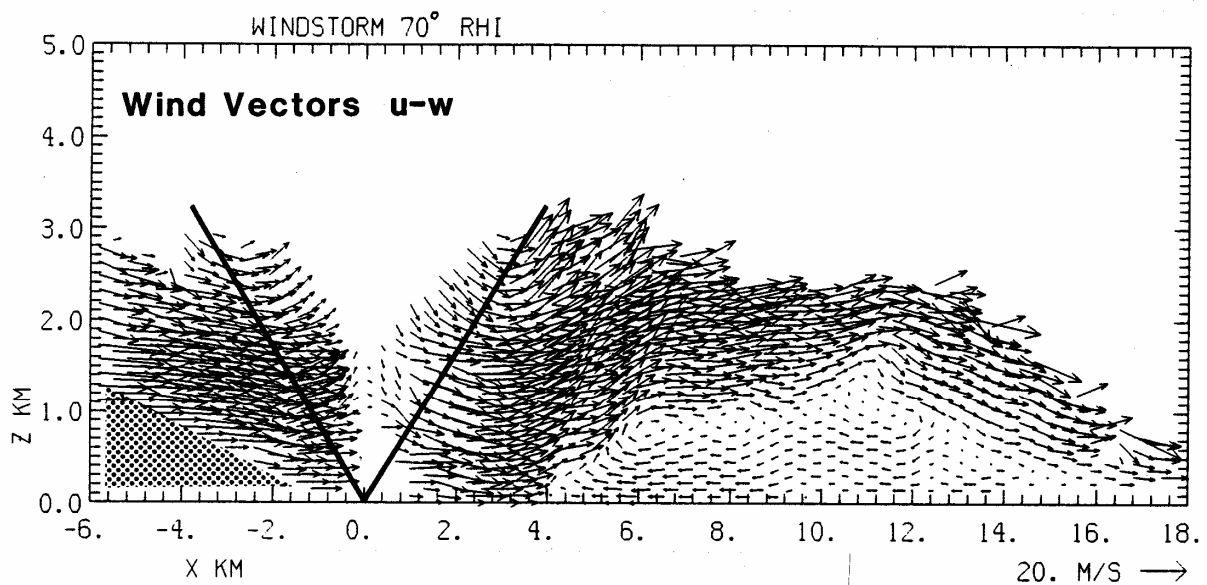


**Figure 7**

Low-level airflow during 9 January 1989 severe downslope windstorm over Boulder, Colorado, as measured by NOAA's Scanning Doppler Lidar. Wind vectors within the cone over the lidar position may be spurious. Note a near-surface flow reversal indicating rotor development at  $x > 4$  km, and sub-rotor vortices aloft at  $x = 6$  km and  $x = 11-12$  km (from Banta et al. 1990).

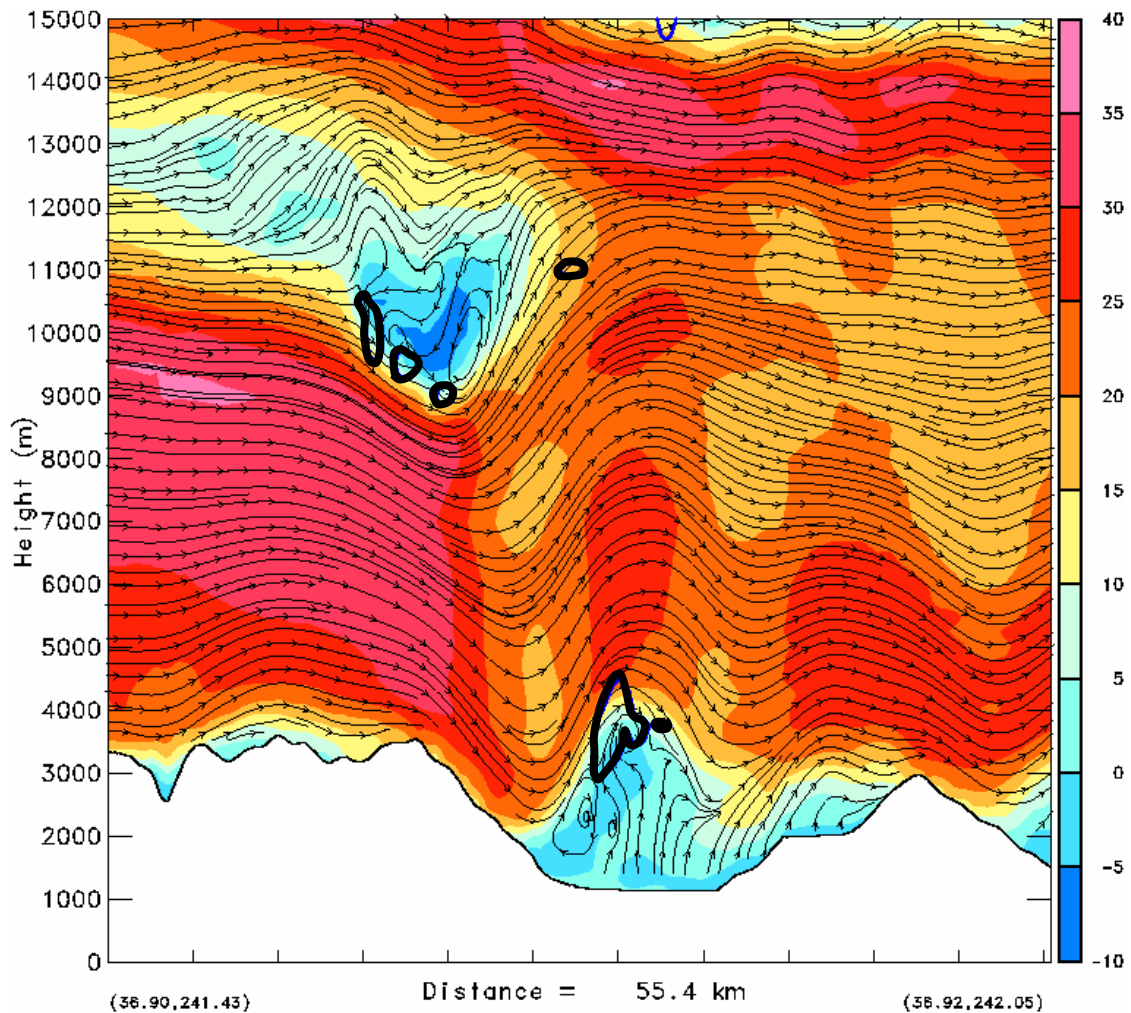


**Figure 8**

Vertical cross section of simulated streamlines and cross-mountain wind component (color scale,  $\text{m s}^{-1}$ ) oriented across the Sierra Range using COAMPS valid at 00 UTC 20 November 1996 (24-h simulation time). The  $20 \text{ m}^2 \text{ s}^{-2}$  turbulence kinetic energy contour is shown by the bold black contour. The simulation used five nested grids with the innermost mesh ( $\Delta x=333 \text{ m}$ ) shown here. A complex low-level rotor circulation is apparent in Owens Valley along with reversed flow aloft associated with wave breaking near 10 km ASL above the Sierra crest. A commercial airline encountered severe turbulence that resulted in an injury near this time and above Bishop, CA at  $\sim 9 \text{ km}$  asl (provided by J. Doyle).

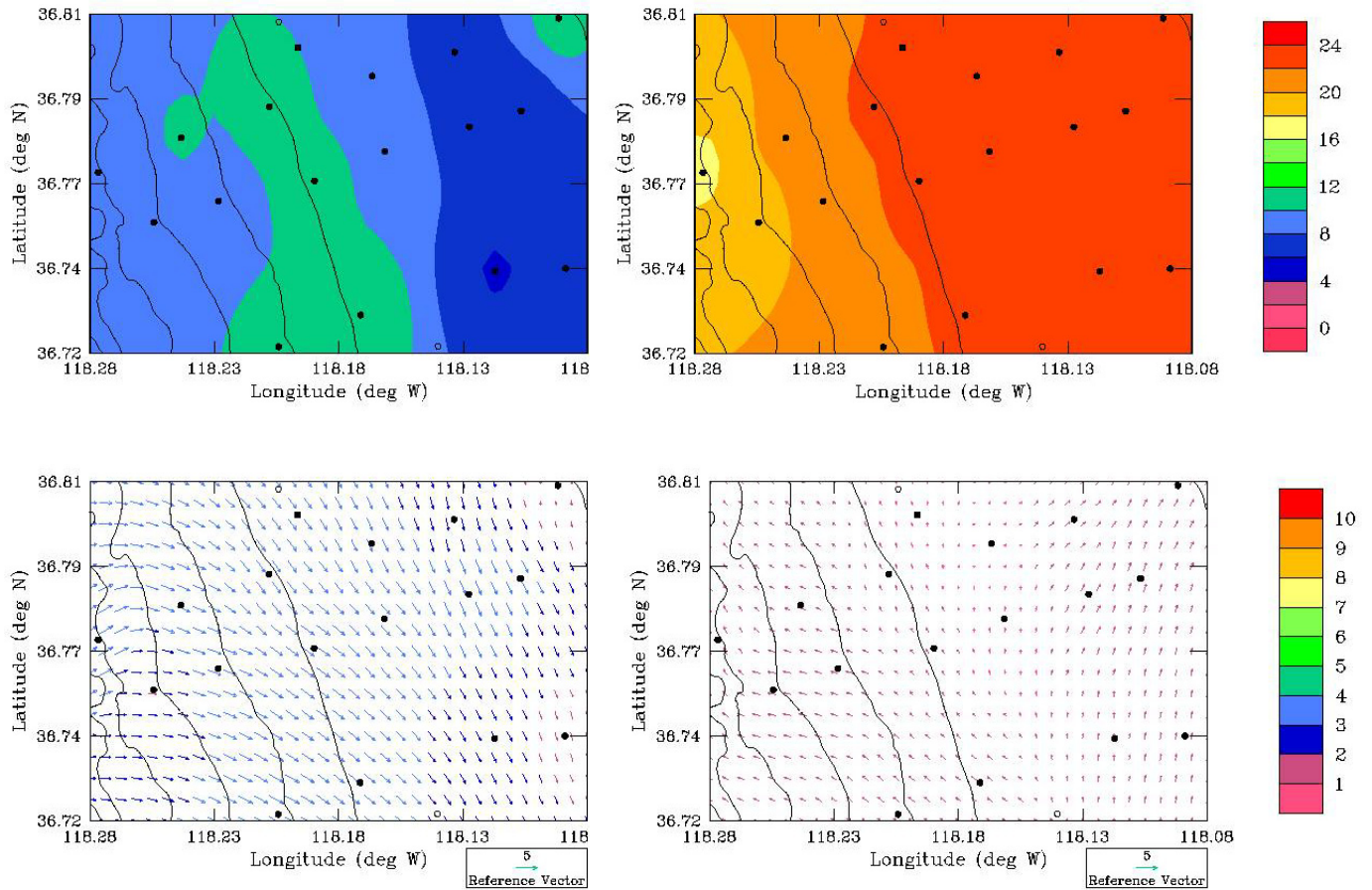


**Figure 9**

Average temperature and circulation over the DRI ground station network area in Owens Valley during March 2004 during Sierra Rotors Project. Black dots indicate AWS locations. Top row: Temperature in degrees C. Bottom row: Wind vectors. At 02 PST, a cold pool (top left) with northerly wind in the valley and downslope flow on the western slope (bottom left). At 15 PST, the highest temperatures are found at the valley floor (top right), with the southerly and upslope winds over the network area (bottom right). (Provided by V. Grubišić from the SRP data).

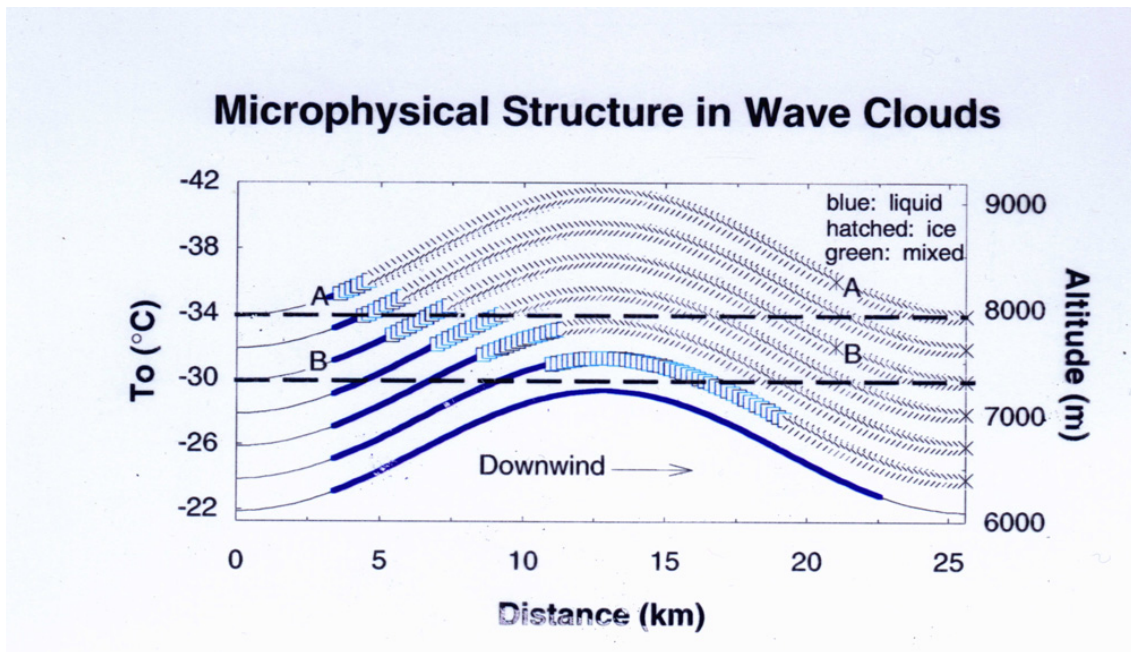


**Figure 10**

Top: Schematic depiction of the phase transition process in a wave cloud (A. Heymsfield). Bottom: Multilayer structure of wave clouds in the lee of the Sierra Nevada. View southward along Owens Valley from about 9 km on 1 May 1955 during the Sierra Wave Project. The rotor (roll) clouds are at about 4.5 km, whereas the highest wave cloud is near 12 km. The original photo has been rotated around its vertical axis to show wind from the left (Photo: T. Henderson).



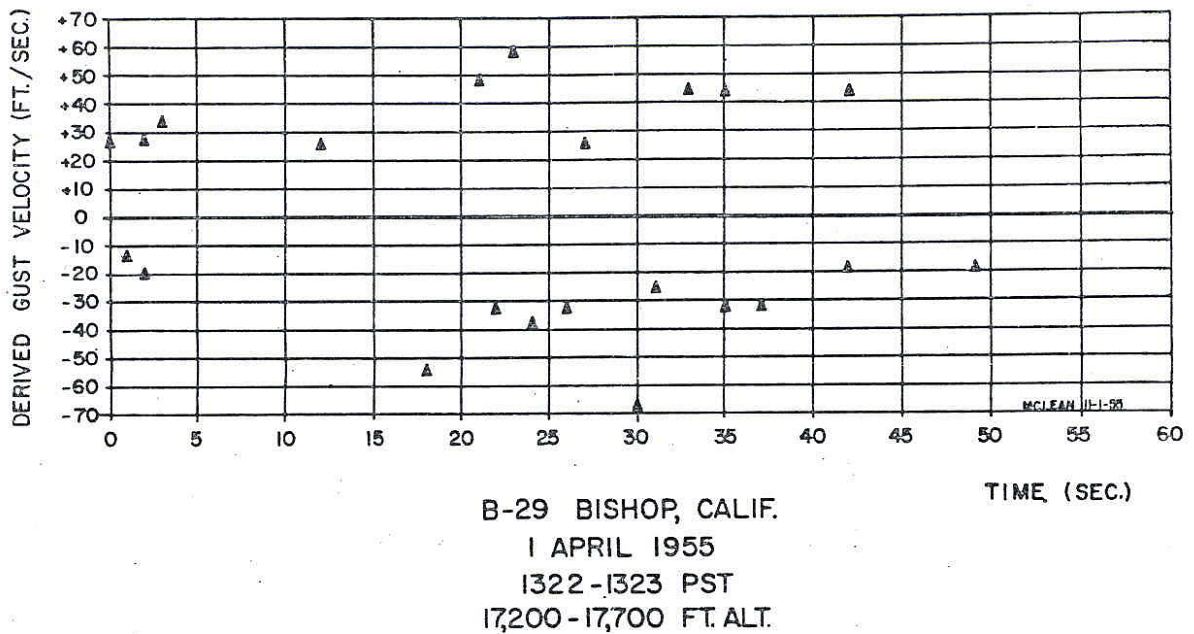
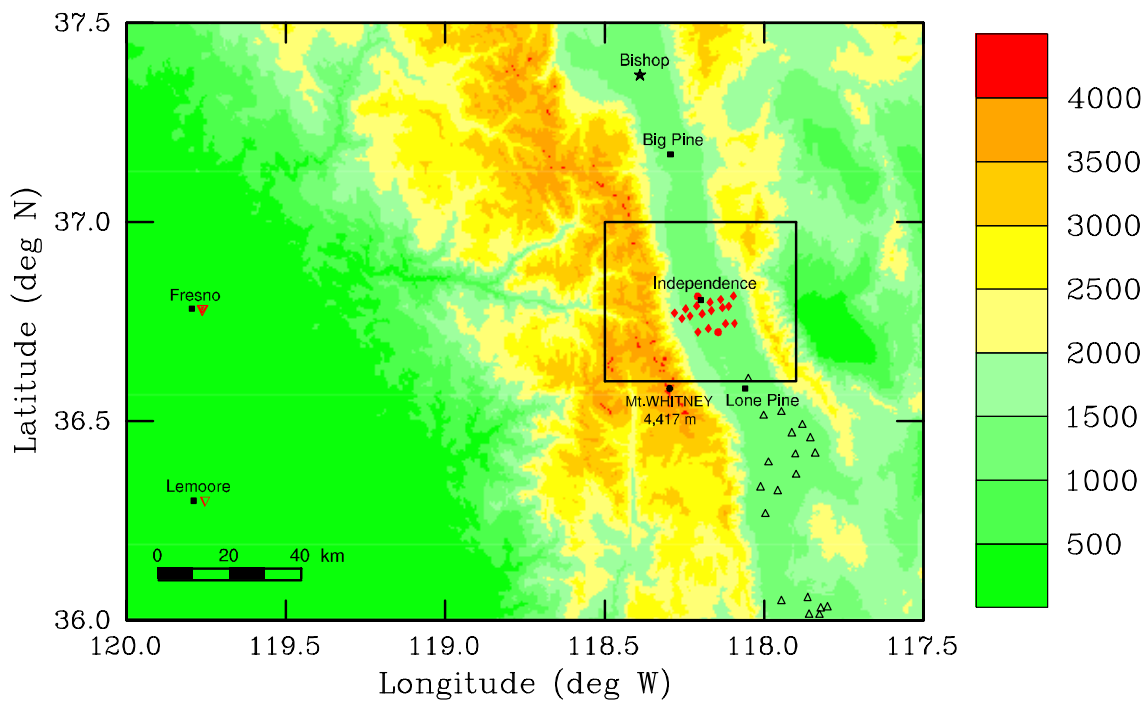


**Figure 11**

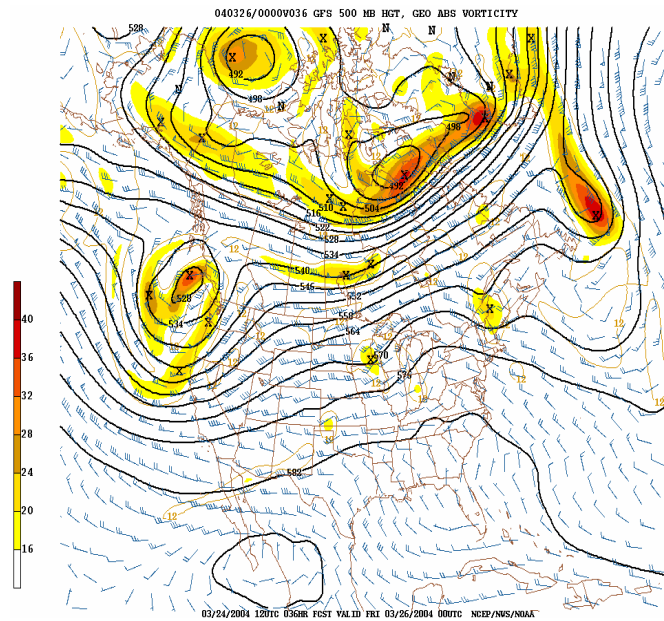
Penetration of a severe rotor by an instrumented B-29 aircraft at 500 hPa level, showing 20 positive and negative vertical gusts reaching  $\pm 20\text{ms}^{-1}$  over less than a minute (from the Sierra Wave Project, Holmboe and Klieforth 1957).



- ★ Operations Center
- ◆ DRI AWS with Telemetry
- NCAR ISS (MAPR, MISS)
- ▽ NCAR MGAOS
- ▽ NAS Lemoore Sounding
- △ GBUAPCD AWS

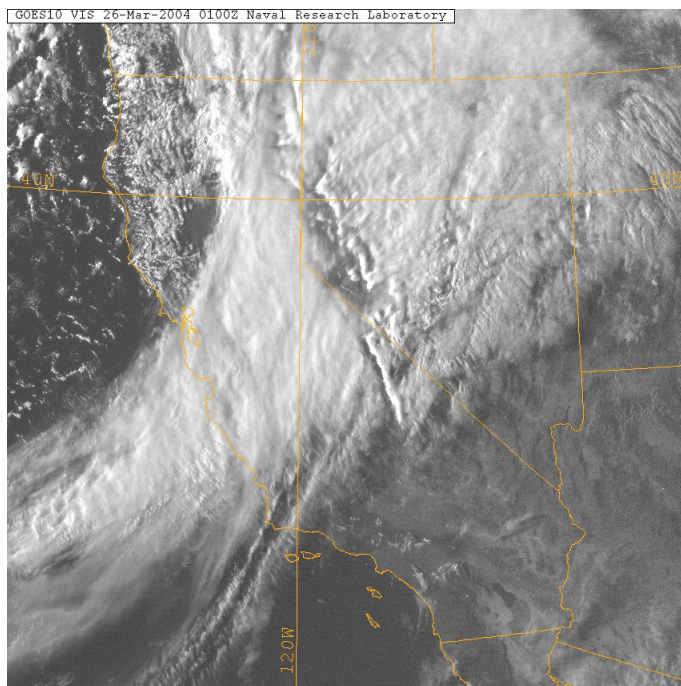
**Figure 12**

Base map of the Sierra Rotors Project (SRP) location and instrumentation. Red symbols show the location of the Sierra Rotors project instrumentation. Shown is also a preexisting network of the Great Basin Unified Air Pollution Control District (GBUSAPCD) automatic weather stations clustered around the dry Owens Lake bed (From Grubišić and Kuettner 2004).



**Figure 13**

Left: NCEP GFS model prediction of wind, geopotential height, and vorticity at 500 hPa for 00 UTC 26 March 2004 during SRP IOP 8 showing a classical prefrontal situation conducive of wave generation in Owens Valley. Bottom left: GOES10 visible satellite image from 01 UTC March 26 (17 PST March 25). Bottom right: A view from the ground of the rotor and wave clouds around 01 UTC March 26. Dust, lofted from the dry Owens Lake bed by strong westerly winds, is visible in the far south. View southeast from the west of Independence (from Grubišić and Cohn 2004; Photo: V. Grubišić).



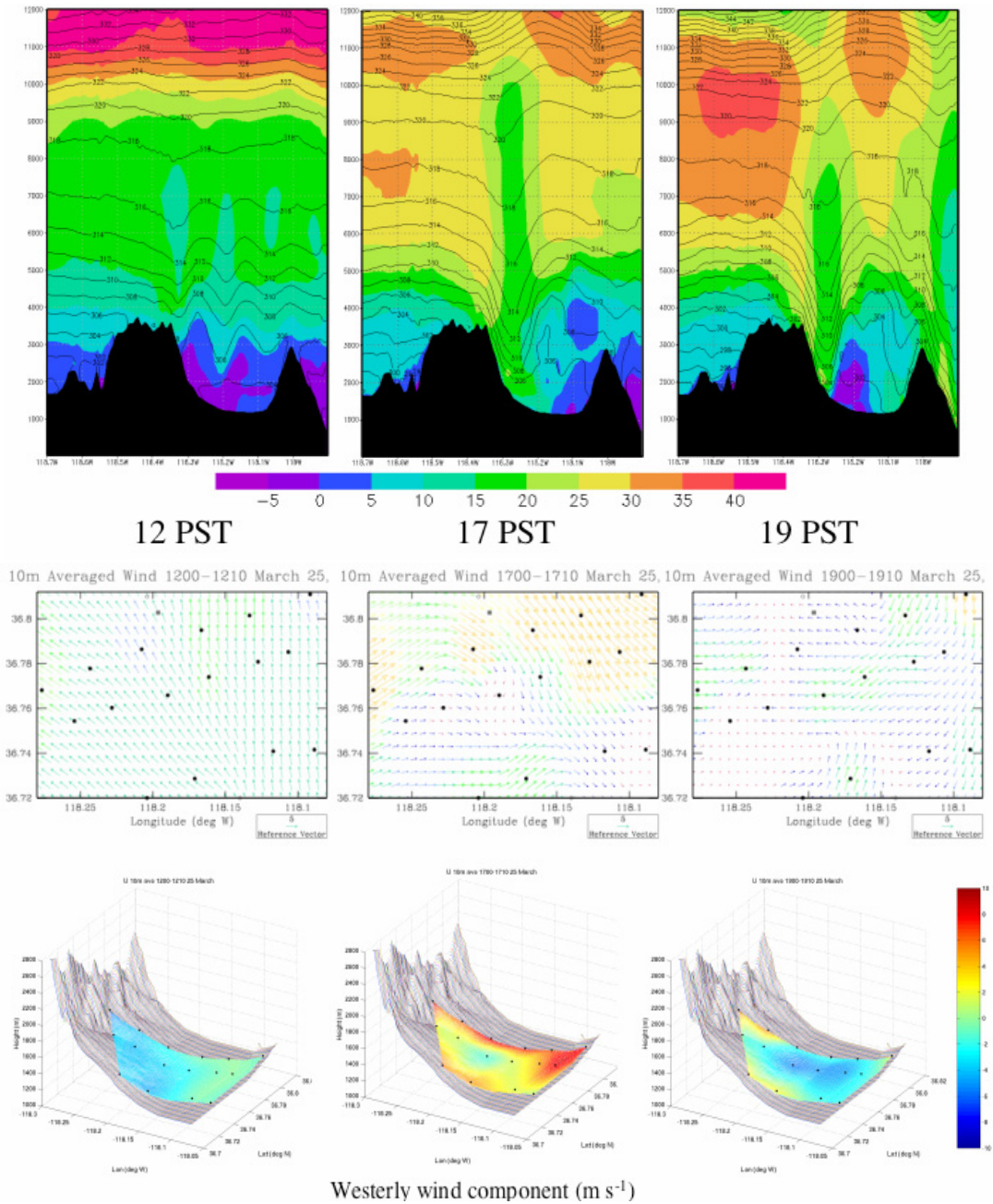


**Figure 14**

Evolution of the mountain wave and rotor during 25-26 March 2004 in SRP IOP 8). Times shown are: March 25, 20 UTC (left), March 26 at 01 UTC (middle) and March 26 at 03 UTC (right). UTC = PST + 8 hours. Top row: Model simulated potential temperature and the westerly wind component in the east-west vertical cross-section through Independence. The cross-section is from the innermost domain (horizontal resolution of 333 m) of a COAMPS simulation with five nested grids. Middle row: Objective analysis of the 10-m wind data measured by the ground network at those times. Bottom: Terrain of Owens Valley surrounding the DRI ground network. The westerly wind component ( $\text{m s}^{-1}$ ) is shown on top of the terrain surface. A ground footprint of a rotor is seen at 19 LST, with a large-amplitude wave and the rotor over Owens Valley, and the downslope flow of  $15\text{--}20 \text{ m s}^{-1}$  over the western slope (from Grubišić 2005).



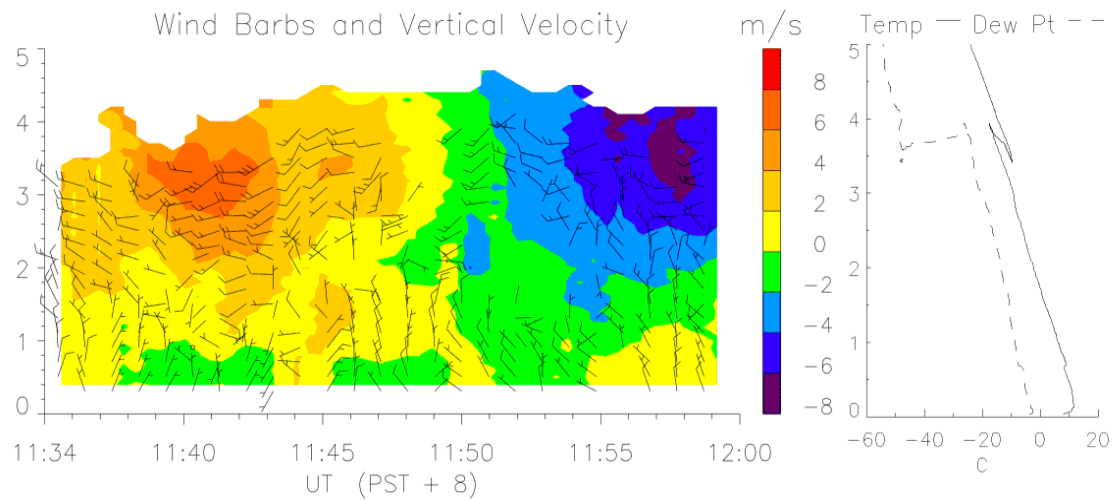


**Figure 15**

Mountain wave as seen by the ISS/MAPR wind profiler (right) and a sounding from Owens Valley from 12 UTC 26 March 2004 obtained during SRP IOP 8 (cf. Figure 14). Note strong up- (red) and down- (blue) drafts documented by the wind profiler. A radiosonde, launched from the ISS/MAPR site, was pulled down about 500 meters into dry warm air by the downdraft (provided by S. Cohn).

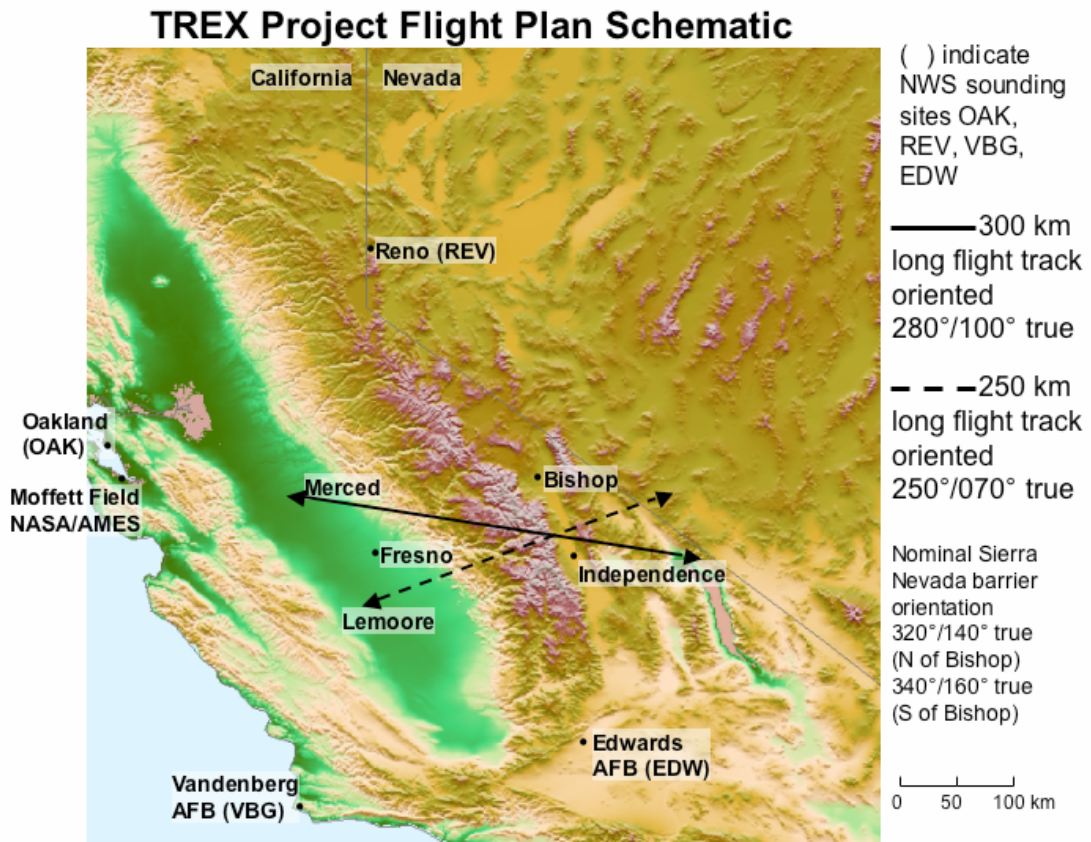


**Figure 16**

T-REX flight-plan schematic showing the orientation of possible cross-mountain flight tracks over the Sierra Nevada and the White-Inyo range. Base map created by the UCAR Joint Office of Scientific Support.

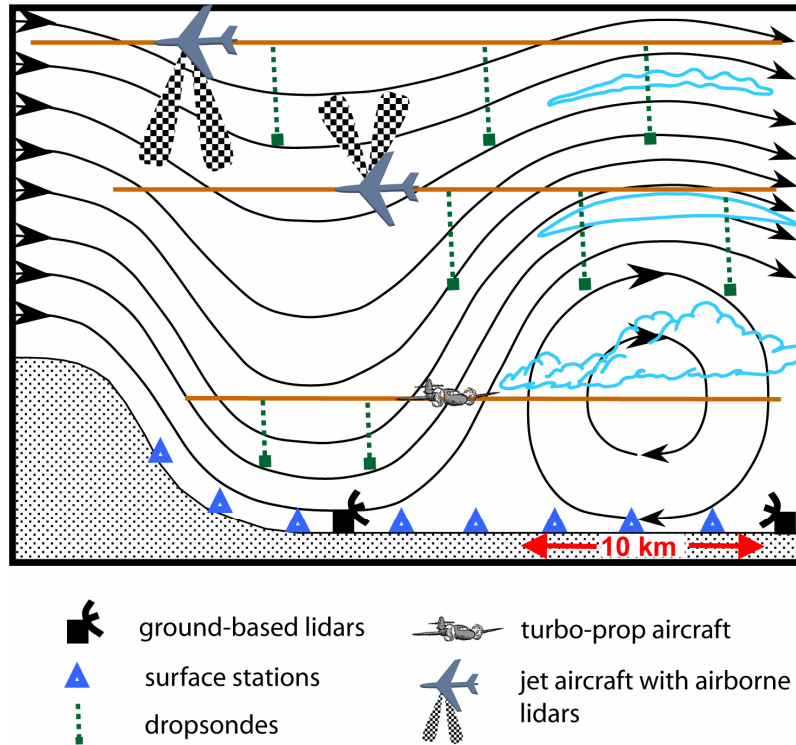
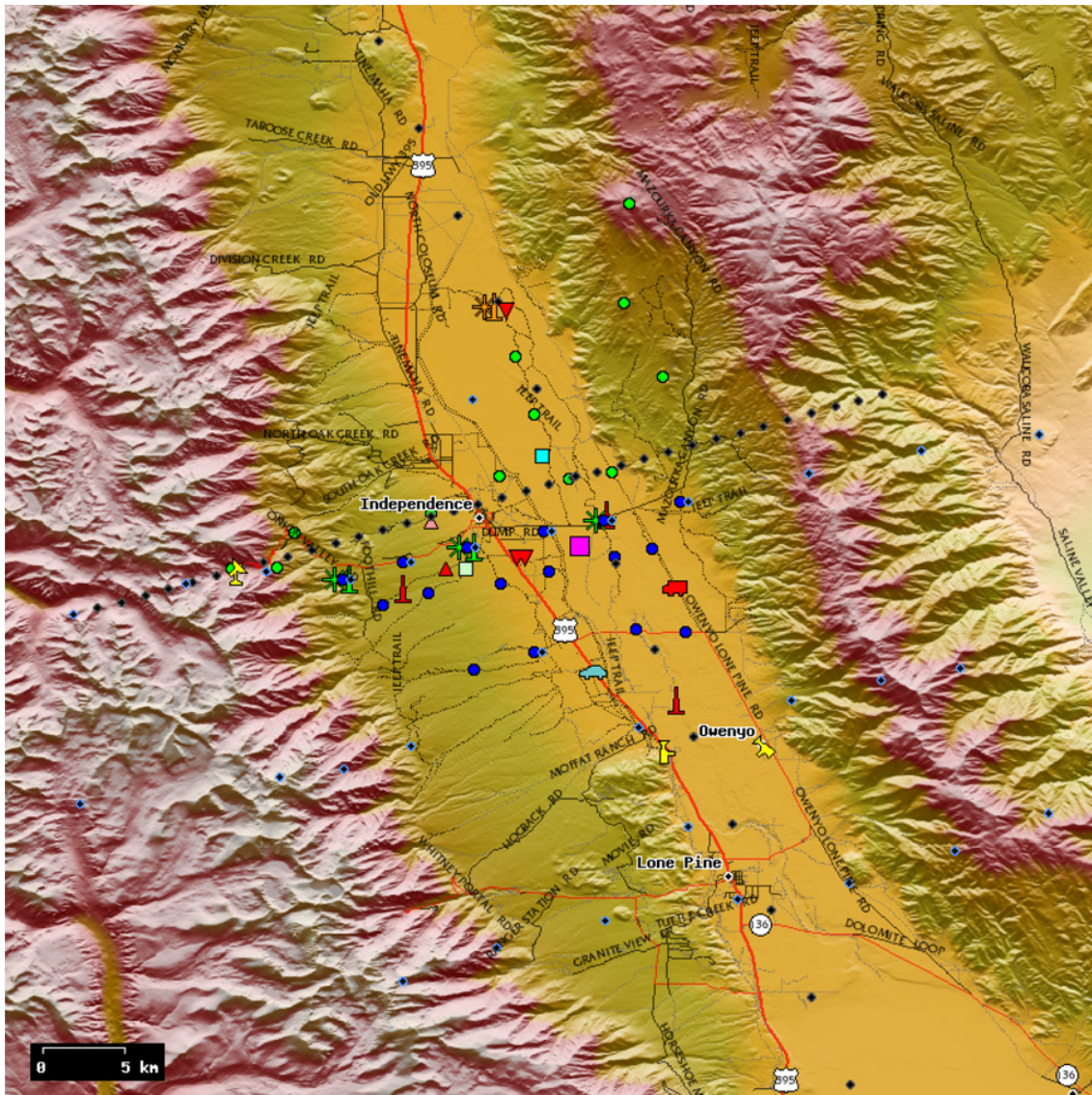


**Figure 17**

Schematic view of a generic T-REX composite observing system showing major instrumentation in approximate relation to the rotor phenomenon (provided by V. Grubišić and J. Doyle).



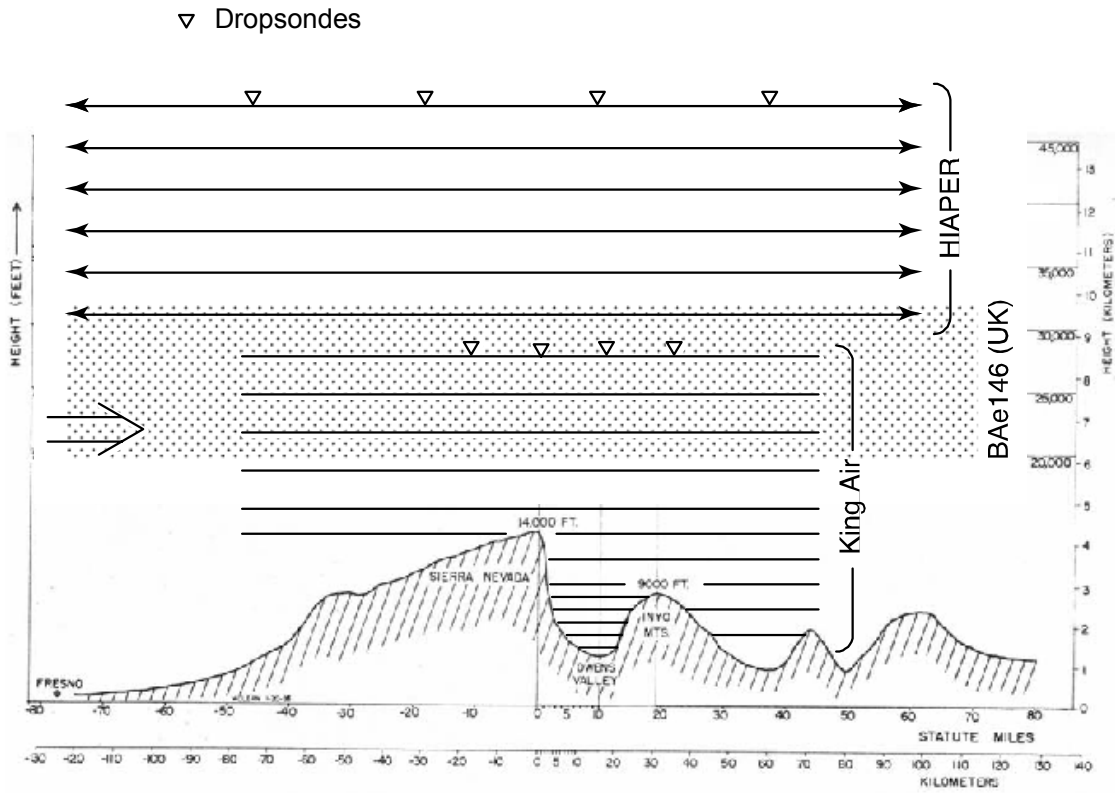


- Yale video cameras
- Yale K-band Radar
- soil moisture
- U. Innsbruck instrumented car
- NCAR MISS
- NCAR ISS
- NCAR ISS MAPR
- GPS sounding site
- MGLASS
- U. Utah HOBOS
- DRI AMS
- U. Leeds AMS
- U. Houston flux tower
- U. Houston sodar
- U. Leeds flux towers
- U. Leeds sodars
- NRL Aerosol Lidar
- NCAR REAL
- ASU Doppler Lidar
- DLR Doppler Lidar
- NOAA Doppler Lidar
- NCAR ISFF

**Figure 18**

Color relief map of the central portion of Owens Valley showing the T-REX field campaign area and the proposed ground-based instrumentation. A GPS sounding site at NAS Lemore (pink diamond) and the MGLASS location (red star) and are expected to be the same as in the Sierra Rotors Project (cf. Figures 12 and 16). The regular NWS upper-air sounding locations in the surrounding area: Oakland, CA, Vandenberg AFB, CA, and Reno, NV are also shown in Figure 16. (Map: V. Grubišić in collaboration with the UCAR Joint Office of Scientific Support.)






**UCAR** Armi and Kuettner

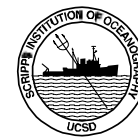


**Figure 19**

Generic cross-mountain flight tracks with drogsonde releases and the vertical range of all three planned aircraft shown in relation to the terrain, in the vertical cross-section whose base line is indicated with a bold dashed line in Figure 16.

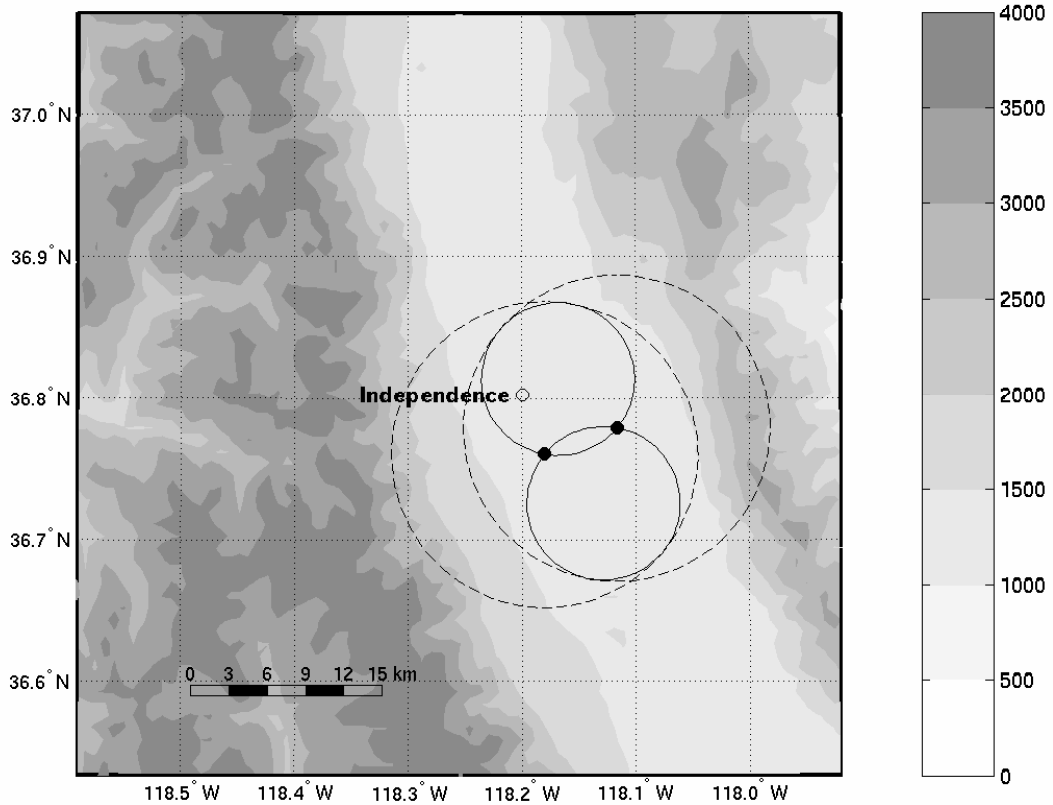


**Figure 20**

Topographic map of Owens Valley surrounding Independence showing a potential configuration for two Doppler lidars (black circles) sited along a line perpendicular to the ridge and valley axes. Dashed circles represent the area of coverage of individual lidars assuming 12-km range. The union of solid circles (minus their intersection) represents an area of overlap for dual-Doppler velocity calculations, where both lidar beams intersect at an angle between  $30^\circ$  and  $150^\circ$ . The area along the baseline, in between the two lidars, is not available for dual-Doppler wind calculations because the angle between the scan planes is too small to provide two accurate horizontal wind components. This particular configuration provides an extended dual-Doppler coverage of along-valley flow variability. Lidars could also be oriented so that their baseline is along the axis of the valley, providing extended dual-Doppler coverage in the cross-valley direction. Additionally, three Doppler lidars could be arranged in a triangle configuration, and, if available, quadruple Doppler lidars, in a square or double triangle configuration, extending the coverage in both the along- and cross-valley directions. (Diagram: D. Durran).

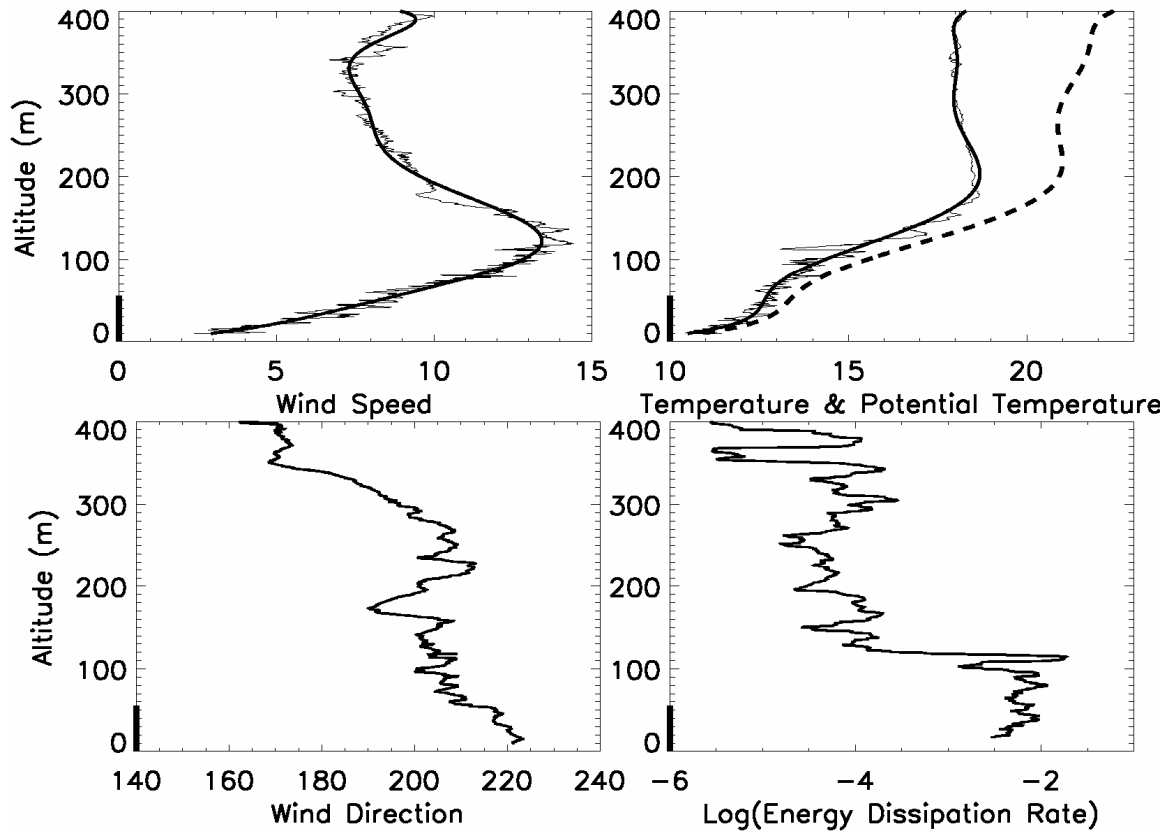


**Figure 21**

High-resolution profiles obtained using the Tethered Lifting System (TLS) in the CASES-99 campaign. Upper panels show profiles of 1 s wind speed (left) and temperature data (right), and the polynomial fitted curves (solid lines). Potential temperature polynomial fit is shown as dashed curve. Lower panels show 20-second smoothed wind direction (left) and 20-second smoothed profile of energy dissipation rate (right). While this figure shows results up to 400 m, the TLS can produce similar results up to  $\sim 3$  km at roughly hourly intervals. The dark vertical line on the left of each panel illustrates the height of a 55 m instrumented tower for reference (provided by B. Balsely).